Fall 2019

# Effect of the Physical Micro-Environment on Cell Adhesion and Force Exertion

Mohamad Eftekharjoo
*Old Dominion University*, mefte001@odu.edu

# EFFECT OF THE PHYSICAL MICRO-ENVIRONMENT ON CELL ADHESION AND FORCE EXERTION

by

Mohamad Eftekharjoo
B.S. August 2011, Azad University, South Tehran Branch
M.S. December 2015, Old Dominion University

A Dissertation Submitted to the Faculty of
Old Dominion University in Partial Fulfillment of the
Requirements for the Degree of

DOCTOR OF PHILOSOPHY

MECHANICAL ENGINEERING

OLD DOMINION UNIVERSITY
December 2019

Approved by:

Venkat Maruthamuthu (Director)

Moustafa Moustafa (Member)

Shizhi Qian (Member)

Oleksandr Kravchenko (Member)

## ABSTRACT


### EFFECT OF THE PHYSICAL MICRO-ENVIRONMENT ON CELL ADHESION AND FORCE EXERTION

Mohamad Eftekharjoo
Old Dominion University, 2019
Director: Dr. Venkat Maruthamuthu

Physical characteristics of the microenvironment, such as geometry and stiffness, influence cell adhesion and contractile forces. Here, we determined how these physical factors influenced cell force exertion and adhesion in two specific contexts that have broad relevance.

Fibroblasts are cells in connective tissues that interact with a fibrous extracellular matrix (ECM) that have a predominantly one-dimensional (1D) (fibrillar) geometry. However, it has been unclear as to how the 1D nature of the fibrillar ECM influences the forces exerted by fibroblasts. Here, we used fibroblast cells adherent on fibronectin lines on polyacrylamide (PAA) gels of stiffness 13 and 45 kPa to restrict the cells in a 1D geometry. We used traction force microscopy (TFM) to quantify fibrillar force exertion by fibroblasts. We found that, even though the cell length depended on substrate stiffness, the exerted force was independent of it. Furthermore, we found that fibrillar fibroblasts display prominent linear actin structures. Accordingly, we found that the cell length and forces exerted by fibroblasts highly depend on the actin nucleator formin. These findings have important implications for disease conditions such as fibrosis.

In epithelial tissues, epithelial cells adhere to the ECM and to neighboring cells to maintain tissue architecture. E-cadherin adhesions bind neighboring cells together, but whether these adhesions respond to surrounding cell-like stiffness is unknown. Here, we developed a biomimetic interface with oriented immobilization E-cadherin with cell-like stiffness to mimic cell-cell binding. We fabricated soft silicones with stiffness in the range of that of epithelial cells (0.4 – 8.7 kPa) (as quantified using rheology) for this purpose. We found that the single cells on stiffer substrates tend to form prominent linear adhesions whereas those on softer substrates are more likely to form just nascent adhesions. The presence of contractile circumferential actin appears to be important for large adhesion formation. We also found that the formation of large E-cadherin adhesions highly depends on the actin nucleator formin, but not Arp2/3. Our biomimetic E-cadherin substrates have thus enabled us to gain insights into the effect of cell-like stiffness on E-cadherin adhesion, which is relevant to understand morphogenesis as well as cancer.

This thesis is dedicated to my parents.

## ACKNOWLEDGMENTS

Foremost, I would like to express my sincere gratitude and deepest appreciation to my advisor Prof. Venkat Maruthamuthu for the continuous support of my Ph.D. study and research, and for his patience, motivation, enthusiasm, and immense knowledge. His guidance helped me in research and the writing of this dissertation.

Besides my advisor, I would like to thank Dr. Moustafa Moustafa, Dr. Shizi Qian, and Dr. Oleksandr Kravchenko for their encouragement and insightful comments.

Finally, I would like to thank my family for supporting me spiritually throughout my life.

**Table of Content**

## LIST OF TABLES

## LIST OF FIGURES

# CHAPTER 1

# INTRODUCTION

Single cells are the simplest units of life on earth. Cells sense their surroundings and respond to their microenvironment in a manner that depends on biochemical, physical and mechanical factors. Cell interaction with its microenvironment crucially influences tissue development, hemostasis, and differentiation. In this chapter, we focus on a broad overview of the fundamental roles of biophysical cues in single cell function. In general, understanding single cell functionality makes it possible to extend our understanding to mechanisms operating in multi-cellular cell collectives.

## 1.1 Cells and the ECM

Adherent cells bind to their extracellular matrix microenvironments and sometimes neighboring cells using cell surface adhesion molecules. This influences whether and how they survive, divide, and migrate. Epithelial tissues are composed of epithelial cells that adhere to each other with junctions such as tight junctions, gap junctions, adherens junctions, and desmosomes. In addition to the cell-cell contact network, epithelial cells also bind to the basement membrane beneath (Figure 1) via adhesions such as focal adhesions and hemi-desmosomes. Basement membrane is the top most layer of connective tissue beneath the epithelial cell layer and is composed of a net-like extracellular matrix (ECM) network. Connective tissues are located between tissues such as muscle tissue, nerve tissue, and epithelial tissue within organs. Fibroblasts are the most common type of cells that are present in connective tissue and interact with the ECM. Physical and biochemical signals from the ECM provide cues for fibroblasts to migrate

[1]. Migration of such cells has four main events: protrusion of the leading edge, formation of new adhesions at cell-ECM interface, cell movement, and retraction of the trailing edge [2]. These aspects of 2D cell migration depend on physical properties of the ECM such as stiffness and ECM concentration [3]. The ECM in 3D is more complex but can be experimentally modelled using reductionist approaches. For instance, Doyle et al, showed that fibroblasts in 1D micropatterrned lines mimic the fibroblasts phenotype in three-dimensional (3D) network of matrix [4].

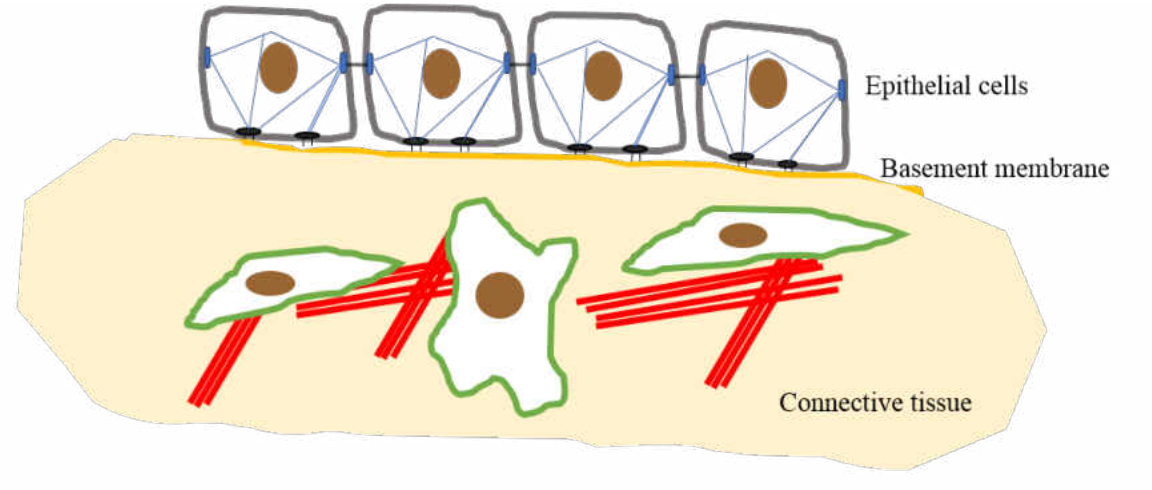


Figure 1. Simplified schematic depiction of epithelial cells on the basement membrane and fibroblast cells located within connective tissue.

**1.2 Topology and mechanical properties of the ECM**

The ECM is a 3D network of fibrous molecules and other non-cellular components that is present in all tissues. The ECM possesses biochemical and biomechanical cues that are required for cell function such as growth, survival, differentiation, and division [5-7]. There are two main classes of ECM: fibrous proteins and proteoglycans. Proteoglycans have a variety of functions including preserving the hydrated state of the ECM as well as

storing growth factors. The main fibrous ECM proteins are collagens, elastins, fibronectins, and laminins. Collagen fibers often constitute the main structural component of the ECM [8]. Elastin fibers are associated with collagens, which provide recoil when tissues undergo stretch [9]. Fibronectins are the fibrous ECM component linked to collagen fibers[10] that are enriched in connective tissues and play roles in cell migration. The effect of ECM composition on cell behavior has been extensively studied [11]. In addition to ECM composition, the physical characteristics of the ECM such as elasticity and rigidity have a profound impact on cell behavior [12, 13]. The main physical characteristics of ECM are ligand density, fiber stiffness, and pore size [14, 15], which influence cell adhesion and migration. Individual fibers such as type-I collagen fibers possess local elastic modulus in MPa range [16]. The collagen fibrils exhibit non-linear mechanical behavior; fibrils are elastic and become stiff under tensile forces. The strength of collagen fibers is a mechanical property that strongly depends on cross-linker molecules. Collagen gels' stiffness is mainly within the range of kPa, depending on water displacement and fibril organization [17]. The collagen fiber concentration as well as their orientation influences bulk collagen stiffness [18].

**1.3 Mechanical properties of cells**

Mechanical characteristics of tissues are among the fundamentally relevant properties influencing tissue function. Tissues are intrinsically viscoelastic in nature and possess different stiffness from Pa to GPa range depending on their location [19]. For instance, brain tissues have elastic modulus of sub to 4 kPa, heart tissues from 5 to 15 kPa and bone tissues with ~ 20 GPa stiffness [20]. Tissue mechanical properties are influenced by both ECM and cell mechanical properties. Many basic components of the cell (such as

plasma membrane, cytoskeleton, and organelles) contribute to its mechanical properties. Atomic Force Microscopy (AFM) is one of the methods that has been used to quantify the stiffness of isolated cells. AFM is a high-resolution technique that utilizes a micron-sized tip connected to a micro-fabricated cantilever beam to deform a sample [21]. To quantify a cell's stiffness, the micron-sized tip of cantilever is pressed against the cell; by knowing cantilever characteristics such as tip geometry and stiffness, the elasticity of the cell can be measured. Such approaches have been used to previously measure the stiffness of fibroblast cells (3T3) [22]. The local stiffness of the fibroblast cells (3T3) varies depending on the cell height. In particular, the higher part of the cells is the softest region whereas the cell edge is stiffer. In addition, stiffness values of normal epithelial cells have been reported [23-25]. It has been shown that older epithelial cells are stiffer than the younger cells [24]. Also, epithelial cells possess different stiffness depending on the part of the cell cycle they are in [25]. For instance, epithelial cells in metaphase are softer than those in anaphase. Even normal epithelial cells' deformability is different from that of malignant epithelial cells. Cancerous epithelial cells are typically softer than normal epithelial cells [26, 27], with a few exceptions such as epithelial prostate cancers which are stiffer and more invasive compared to non-invasive prostatic epithelial cells [28].

**1.4 Integrins as mechanosensors**

It has been shown through multiple studies that cells can detect and respond to the biophysical properties of their microenvironment through integrin receptors. Integrin is a cell adhesion molecule and heterodimer transmembrane receptor protein, which is composed of α and β subunits. Integrins are found in many cell types such as endothelial,

fibroblast, and epithelial cells. There are 24 different types of integrin, each of which is specific to certain ECM types [11]. Integrin adheres to ECM, transmits force and transduces the force (which is dependent on the mechanical nature of the micro-environment) to specific biochemical signals (the latter is called mechanosensing). The extracellular domain of integrin binds extracellular matrix proteins and its intracellular domain links to the actin cytoskeleton through the binding of other proteins in the adhesion (called focal adhesion). The actin cytoskeleton consists of actin filaments, which are polymers of the protein actin. The actin cytoskeleton regulates the morphology of cells in general [29]. Focal adhesions consist of a cluster of proteins (such as vinculin, paxillin, talin etc), which transmit cytoskeletal tension and link the actin filaments to integrins. Integrin ligation triggers its conformational change as well as activation of signaling cascades that lead to actin cytoskeleton assembly and recruitment of other focal adhesion components [30]. In particular, receptor binding to ECM activates the Ras homolog gene family member A (RhoA) through Rho-GTPase phosphorylation [31]. RhoA induces actin filament assembly and myosin light chain kinase (MLCK) activation by activating the formin mDia and ROCK respectively. Here, mDia promotes actin assembly by nucleating actin monomers to form actin filaments. Activation of ROCK phosphorylates MLCK, which enhances actin and myosin linkage to assemble the actomyosin apparatus. In particular, the actomyosin structures generate cellular forces and such forces are transmitted by focal adhesion proteins. Integrins, as mechanical linkers between cell and the ECM, are involved in substrate rigidity sensing and also regulate cell morphology [13]. Cell contractile force generated by actomyosin plays a key role in integrin sensing of substrate stiffness [32]. For example, cells on stiffer substrates

possess larger actin networks, which correspond to larger forces transmitted at integrin-ECM interface [33, 34]. Such increases in cellular force triggers the recruitment of focal adhesion proteins such as vinculin [35]. In addition, cell morphology as well as cell migration are regulated by sensing the microenvironmental stiffness through integrins. Many studies have shown that cells on stiffer substrates adapt to a larger spreading area [33, 36, 37]. Furthermore, studies have developed techniques to probe the tension at single integrin-ECM bonds which is about 40 pN [38]. The molecular tension at integrin-ECM bonds influences the cell spread area - cells with larger molecular tension possess a larger spreading area [39].

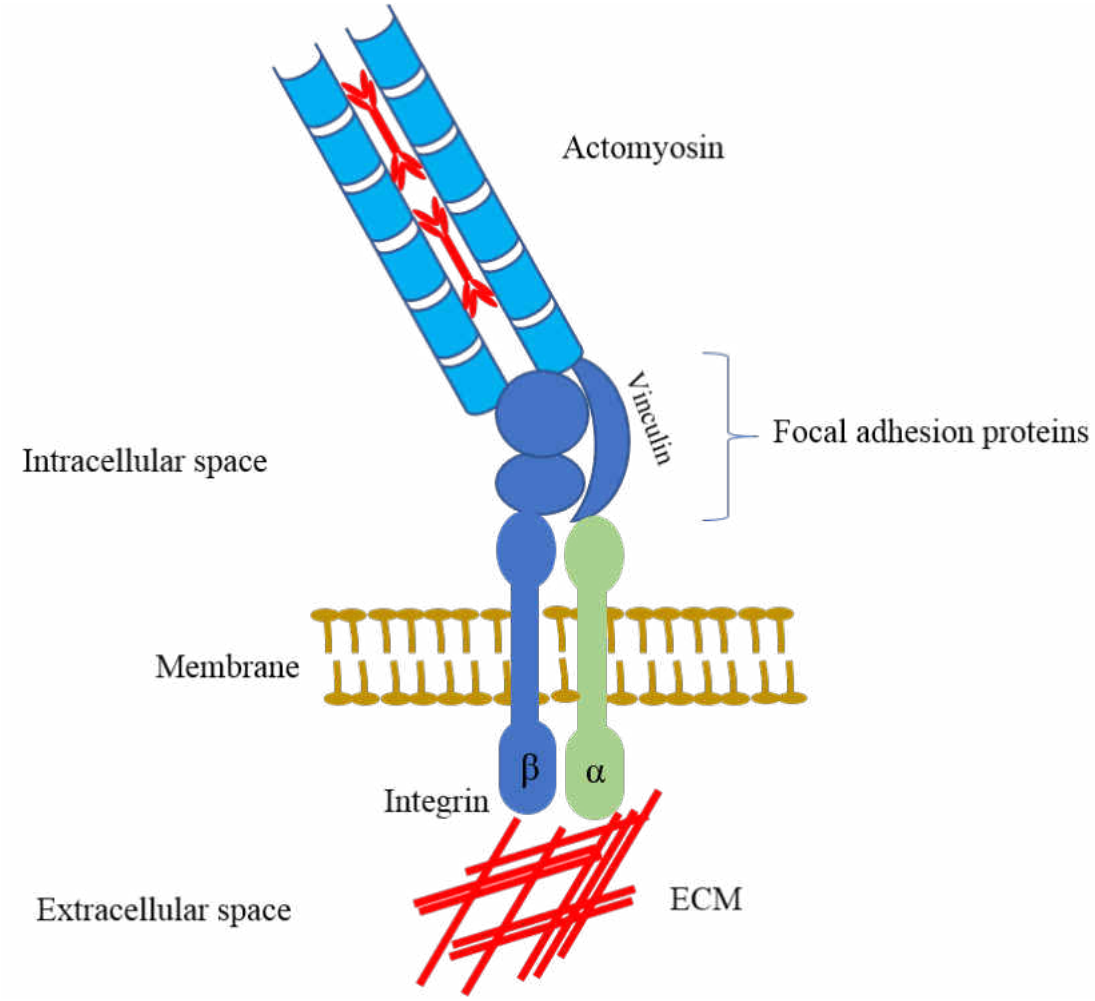

Figure 2. Schematic depiction of integrin and associated proteins in the focal adhesion linked to the actomyosin apparatus.

**1.5 Cadherins as mechanosensors**

In addition to the cell-ECM interface, cells (such as epithelial cells) adhere to each other via cell-cell junctions which maintain tissue integrity. Dynamic adhesions within cell-cell junctions enable cell-cell contacts to be maintained and remodeled [40]. Cadherins are the $Ca^{2+}$-dependent homodimer transmembrane proteins that adhere to cadherins of adjacent cells. The extracellular domain of cadherins bind to the extra-cellular domain of cadherins of adjacent cells whereas its intracellular domain binds to the catenin complex and p120-catenin shown in figure 3. Cadherins are expressed in epithelial (E-cadherin), endothelial (VE-cadherin), and neural (N-cadherin) tissues. Like integrins, cadherins are also connected to actin (through the catenin complex) and the tension exerted via cadherins is ultimately generated by the actomyosin apparatus. Assembly and stability of cadherin adhesions are highly dependent on myosin II activity. Cadherins also modulate cell morphology by organizing actin filaments [41]. Contractility of endothelial cells on substrates of different stiffness dictates gap formation between endothelial cells [42]. During morphogenesis, the forces transmitted by cadherins determine cell and tissue shape [41]. Cadherin adhesions are regulated by physical cues. In particular, the formation of cadherin adhesions depends on the external physical microenvironment [43]. Studies have shown that cellular traction forces transmitted by cadherin enhances with increase in substrate stiffness [44-46]. Alternatively, studies have shown that application of exogenous force to cadherins enhances their recruitment at adherens junctions. Furthermore, application of exogenous torque via cadherin coated magnetic

beads, leads to junction stiffening [44].

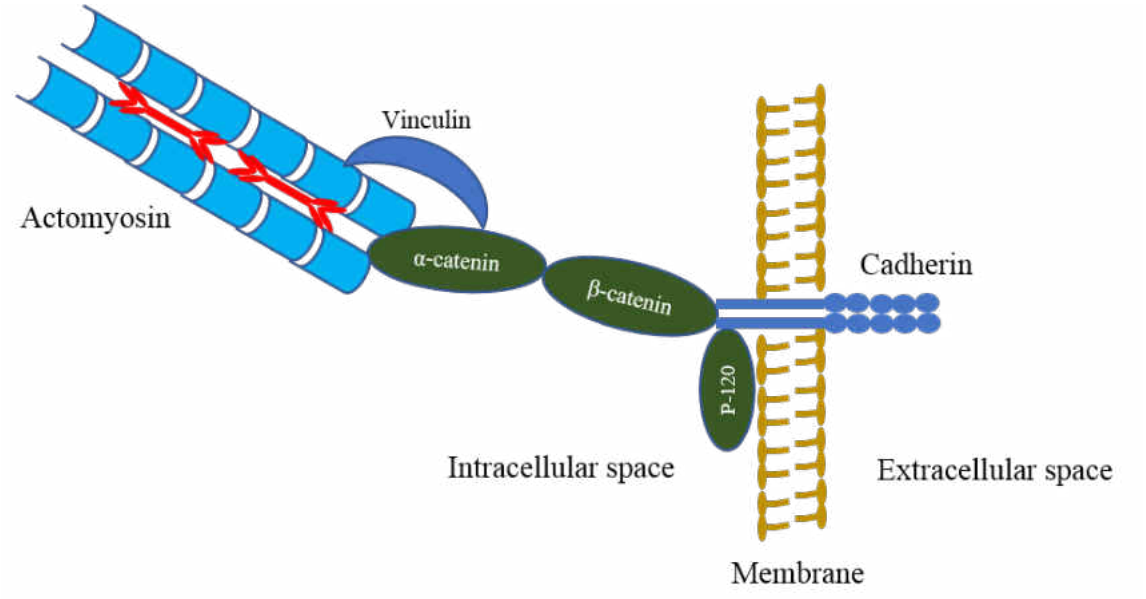


Figure 3. Schematic depiction of E-cadherin at the cell surface and its linkage to the actomyosin apparatus.

**1.6 Biomimetic experimental models to control for geometry, stiffness and adhesion**

Cells interact with their microenvironment in order to survive, migrate, and differentiate. Physical factors such as cell geometry and the stiffness of the microenvironment have been of particular interest, in their modulation of cellular contractility. In order to control the microenvironment stiffness, linear elastic isotropic materials such as polyacrylamide (PAA) hydrogels and cross-lined silicone gels are mainly used as substrates. Their stiffness can be tuned by systematic variation of their composition. Cells have been known to exert different levels of traction forces depending on the substrate stiffness [12]. This is partly due to different cell spread areas on different stiffness substrates. Therefore, micro-patterning methods have been implemented to control the cell geometry. Previous studies have implemented different micro-patterning techniques to

better characterize cellular contractility under different topological constraints using PAA gels and micropost arrays [36, 47]. In addition to physical factors, chemical factors such as ECM composition influences cell function. Recent studies have shown that ECM ligand type influences cellular contractility for the same substrate stiffness [48].

### 1.7 Quantification of cell exerted forces (traction force microscopy)

Adherent cells have physical interactions with their microenvironment by sticking via their adhesions and also exert contractile force onto their substrates through them. Traction force microcopy (TFM) is one of the quantitative methods to measure the cellular force exerted on elastic substrates [49]. In this method, fluorescent marker beads are embedded in a soft substrate such as PAA gel or soft silicone. Cells, by exerting forces onto the substrate (Figure 4A), cause substrate deformation. To capture the substrate deformation, the bead displacement field is obtained by comparing the positions of the displaced beads (due to cell force exertion) against a reference image of undisplaced beads (Figure 4B). The traction force field is computed out of the displacement field by employing elasticity theory [50]. According to Boussinesq, $X = G\mathrm{F}$ in which G and X are the known green function and displacement vector fields respectively. In order to solve the equation for traction force (F), Fourier Transform Traction Cytometry (FTTC) is implemented. Using the FTTC method, traction forces are solved in Fourier space and the traction force values are then calculated by applying an

inverse Fourier transform.

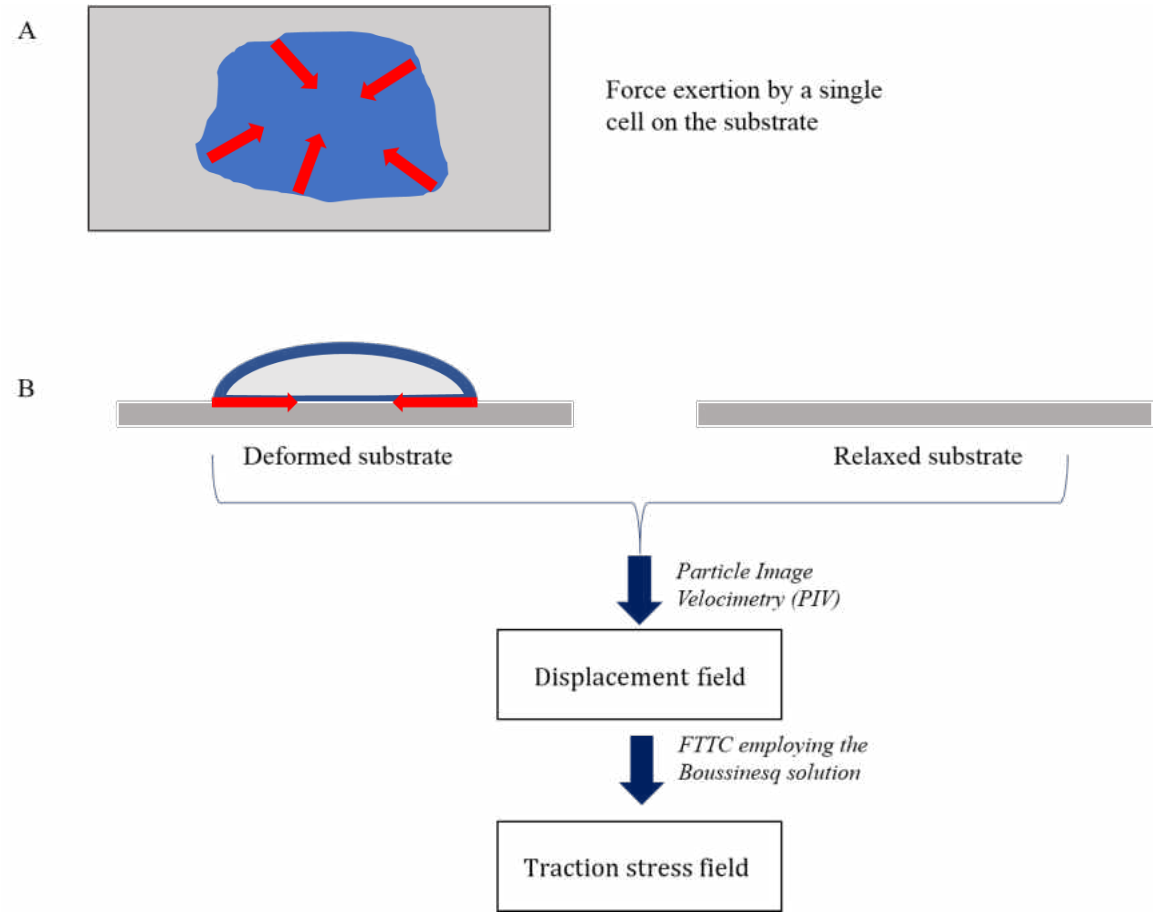


Figure 4. Schematic depiction of traction force microscopy. (A) Top view of single cell on the substrate with fluorescent marker beads. The red arrows are the contractile forces applied by the cell on the substrate. (B) Key steps involved in traction force microscopy.

# CHAPTER 2

## FIBRILLAR FORCE GENERATION BY FIBROBLASTS DEPENDS ON FORMIN

*Note: Contents of this chapter has been published in the journal Biochemical and Biophysical Research and Communications* (*Biochem. Biophys. Res. Commun. 510: 72-77.) by the authors: Mohamad Eftekharjoo, Dakota Palmer, Breanna McCoy, and Venkat Maruthamuthu*


### Abstract

Fibroblasts in the extra-cellular matrix (ECM) often adopt a predominantly one-dimensional fibrillar geometry by virtue of their adhesion to the fibrils in the ECM. How much forces such fibrillar fibroblasts exert and how they respond to the extended stiffness of their micro-environment comprising of other ECM components and cells are not clear. We use fibroblasts adherent on fibronectin lines micropatterned onto soft polyacrylamide gels as an *in vitro* experimental model that maintains fibrillar cell morphology while still letting the cell mechanically interact with a continuous micro-environment of specified stiffness. We find that the exerted traction, quantified as the strain energy or the maximum exerted traction stress, is not a function of cell length. Both the strain energy and the maximum traction stress exerted by fibrillar cells are similar for low (13 kilopascal) or high (45 kilopascal) micro-environmental stiffness. Furthermore, we find that fibrillar fibroblasts exhibit prominent linear actin structures. Accordingly, inhibition of the formin family of nucleators strongly decreases the exerted traction forces. Interestingly, fibrillar cell migration is, however, not affected under formin inhibition. Our results suggest that

fibrillar cell migration in such soft microenvironments is not dependent on high cellular force exertion in the absence of other topological constraints.

**Keywords**: extra-cellular matrix; traction force; micropatterning; actin nucleation; mechanobiology; fibrosis

**Abbreviations:**ECM, extra-cellular matrix; 1D, one-dimensional; 2D, two-dimensional; 3D, three-dimensional; PAA, polyacrylamide; EDC, 1-ethyl-3-(3-dimethylaminopropyl) carbodiimide hydrochloride; sulfo-NHS, N-hydroxysulfosuccinimide

## 2.1 Introduction

Physical cues fundamentally influence multiple aspects of cell function including survival, migration, proliferation, and differentiation [51]. Among physical cues, cell geometry is a key factor that dictates how cells interact with their micro-environment, mainly by its influence on forces generated and transmitted by the cells themselves [52, 53]. Cells embedded in three-dimensional (3D) extra-cellular matrix (ECM) microenvironments, such as fibroblasts, encounter ECM of complex topology [54]. It has been demonstrated that reductionist one-dimensional (1D) fibrillar micro-environments capture key aspects of 3D matrices wherein fibroblasts are often adherent along fibrils in the matrix [4]. Forces generated by cells adherent on 1D fibrils and aligned matrices can be transmitted over long distances and effect changes in the micro-environment that includes other cells [55]. Previous studies have elucidated how fibrillar cell geometry can lead to altered migration rates, compared to a two-dimensional (2D) context [56]. However, despite recent advances [57], the factors that influence force exertion by fibrillar cells have been largely unclear.

Recent approaches with micro-patterned lines and individual suspended fibrils have provided important insights into fibrillar cell migration [58, 59]. However, even when fibroblasts are predominantly constrained in a 1D geometry (adherent on fibrils), they interact with an extended microenvironment consisting of other entangled fibrils, other ECM constituents and cells. While cells in 2D respond to altered stiffness by transmitting altered traction forces [12], it is unclear if cells constrained in 1D geometries can sense surrounding micro-environmental stiffness similarly and modulate transmitted forces [60]. The micro-environmental stiffness encountered by fibroblasts changes during progression of disease states like fibrosis [61]. Thus, it is important to ascertain whether such stiffness cues impact force generation by fibroblasts, which may in turn further modify micro-environmental stiffness in a positive feedback loop.

Previous reports have proposed distinct roles for actin nucleators in fibrillar cell migration [62], but their contribution to fibrillar force generation has not been directly tested. In particular, formin nucleators give rise to prominent linear actin structures in cells [63], but their role in enabling fibrillar cell force generation is unclear. In this paper, we introduce an *in vitro* experimental model that employs micropatterning on soft substrates to quantify force exertion by fibroblasts in a fibrillar (1D) geometry, and test its dependence on microenvironmental stiffness and actin nucleation by formin. We also assess whether fibrillar cell migration speeds relate to the level of fibrillar force exerted by fibroblasts.

## 2.2 Materials and Methods

### 2.2.1 Cell culture

NIH 3T3 cells were cultured in Dulbecco's modified Eagle's medium (Corning Inc., Corning NY) supplemented with L-glutamine, sodium pyruvate, 1% Penicillin/streptomycin, and 10% fetal bovine serum (Corning Inc., Corning NY) at 37 $^0$C, under 5% $CO_2$. For plating micro-patterned polyacrylamide (PAA) hydrogels, about $10^5$ cells were plated in 35-mm culture dishes with a micro-patterned hydrogel-coated coverslip and the medium was replaced within 0.5 hours after plating.

### 2.2.2 Preparation and micropatterning of polyacrylamide hydrogel substrates

PAA gels were made with acrylamide to bisacrylamide ratios of 7.5%:0.1% and 12%:0.1% to yield gels of Young's moduli 13±1 and 45±4 kPa, respectively. The stiffness of the gels was characterized with a Bohlin Gemini parallel plate rheometer (Malvern Instruments, Worcestershire, UK). The gels were doped with red fluorescent beads of diameter of 0.44μm (Spherotech Inc., Lake Forest, IL) to act as fiducial markers. Micropatterning of the PAA gels were performed as follows [52]: a quartz photomask coated with chrome except for clear lines of 1.5 μm width (Toppan, Round Rock, TX) was cleaned with isopropanol and then wiped with toluene. Then, ~100 μL of a acrylamide/bisacrylamide polymerizing mixture [64-66] was placed on the chrome side of the photomask and sandwiched with a 22 × 22 mm$^2$ glass coverslip (Corning Inc., Corning NY) that had been pre-activated by treating with 2% 3-aminopropyltrimethyoxysilane and 1% glutaraldehyde. After PAA gel polymerization, the gel on the mask was exposed to deep UV light (through the mask) for 2.5 minutes. The PAA gels were then incubated with an

aqueous solution with 10 mg/ml each of EDC (1-ethyl-3-(3-dimethylaminopropyl) carbodiimide hydrochloride) and sulfo-NHS (N-hydroxysulfosuccinimide) for 25 min at room temperature. This was followed by incubation with 0.01 mg/ml of fibronectin (Millipore Sigma, Burlington, MA) in 100 mM sodium biocarbonate, pH 8.5 for 30 min. After a few washes with PBS, cells were plated on the PAA gels and imaged about 16 hours later.

### 2.2.3 Live cell imaging and immunofluorescence

Live and fixed cells were imaged using a Leica DMi8 epifluorescence microscope (Leica Microsystems, Buffalo Grove, IL) equipped with a $10 \times 0.3$ NA objective and a Clara cooled CCD camera (Andor Technology, Belfast, UK). An airstream incubator (Nevtek, Williamsville, VA) was used to maintain the temperature at 37 $^{0}$C during time lapse imaging of live cells. Cells were fixed with 4% paraformaldehyde (Electron Microscopy Sciences, Hatfield, PA) with 1.5% Bovine Serum Albumin and 0.5% Triton. Alexa-488 conjugated phalloidin was from Thermo Fisher Scientific, Waltham, MA. To quantify cell migration speeds, time lapse images of 3T3 cells (on patterned lines on the PAA gel) were acquired every 10 min over a duration of 2 hours. Using ImageJ, the cells were manually tracked to locate their position every 10 min. The average cell speed was the sum of the magnitudes of cell displacement every 10 min over 2 hours, divided by the total time (2 hours).

### 2.2.4 Traction force microscopy

First, fibrillar cell phase images and bead fluorescence images, as well as bead fluorescence images after cell detachment (using 10% sodium dodecyl sulfate) were obtained. After

image alignment using ImageJ [67], the displacement field was computed using MATLAB (MathWorks, Natick, MA), with code available at http://www.oceanwave.jp/softwares/mpiv/. Traction forces were then reconstructed using regularized Fourier transform traction cytometry which employs the Boussinesq solution [68-72]. The traction exerted was characterized using two metrics: (i) the strain energy stored in the substrate given by $\frac{1}{2}\sum \boldsymbol{T}_i \,.\, \boldsymbol{u}_i$ where $\boldsymbol{T}_i$ and $\boldsymbol{u}_i$ are the traction force and displacement vectors at position *i*, respectively and (ii) the maximum traction stress $\boldsymbol{T}_{max}$, which is the maximum of the magnitudes of all traction stress vectors $\boldsymbol{T}_i$ associated with a given cell.

### 2.2.5 Pharmacological Inhibition and siRNA treatment

Pan-formin inhibitor SMIFH2 was from Millipore Sigma, Burlington, MA. NIH 3T3 already plated overnight on fibillar micro-patterns were treated with 20 μM SMIFH2 for 4 hours prior to live cell imaging.

### 2.2.6 Statistical analysis

For statistical comparisons, two-tailed student's t-test was used with $p<0.01$ considered significant ('*' = $p<0.01$ and '**' = $p<0.001$).

## 2.3 Results and Discussion

We wanted to employ an experimental model that would restrict fibroblast adhesion to 1D but simultaneously enable them to mechanically interact with a soft micro-environment of defined stiffness. It has been previously shown [4] that lines more than a couple of μm in width increasingly mimic 2D cell morphologies and that a line width of 1.5 μm enables

fibrillar cell morphology. We therefore micro-patterned 1.5 μm-wide lines of fibronectin on PAA gels of defined stiffness (Young's modulus 45 kPa), plated NIH 3T3 fibroblast on them and allowed the cells to adhere to the lines overnight (Figure 5A,B). NIH 3T3 cells adhered only to the fibronectin lines and adopted a 1D fibrillar morphology (Figure 5C), consistent with previous reports [4, 62, 73]. We then determined the traction forces exerted by the single cells adherent on single fibronectin lines on the PAA gel. Figure 4C shows the traction stress vectors overlaid on a fibrillar cell image and figure 5D shows the heatmap representation of the traction stress field. The traction stress is mainly localized at the two ends of the cell, consistent with recent reports [60, 73, 74]. Figure 5E,F show how two metrics associated with the exerted traction strain energy, and maximum traction stress varies with cell length. It is evident that there is no clear correlation between either traction metric and the cell length, in contrast to what has been observed in wider lines [73] and 2D [52, 53].

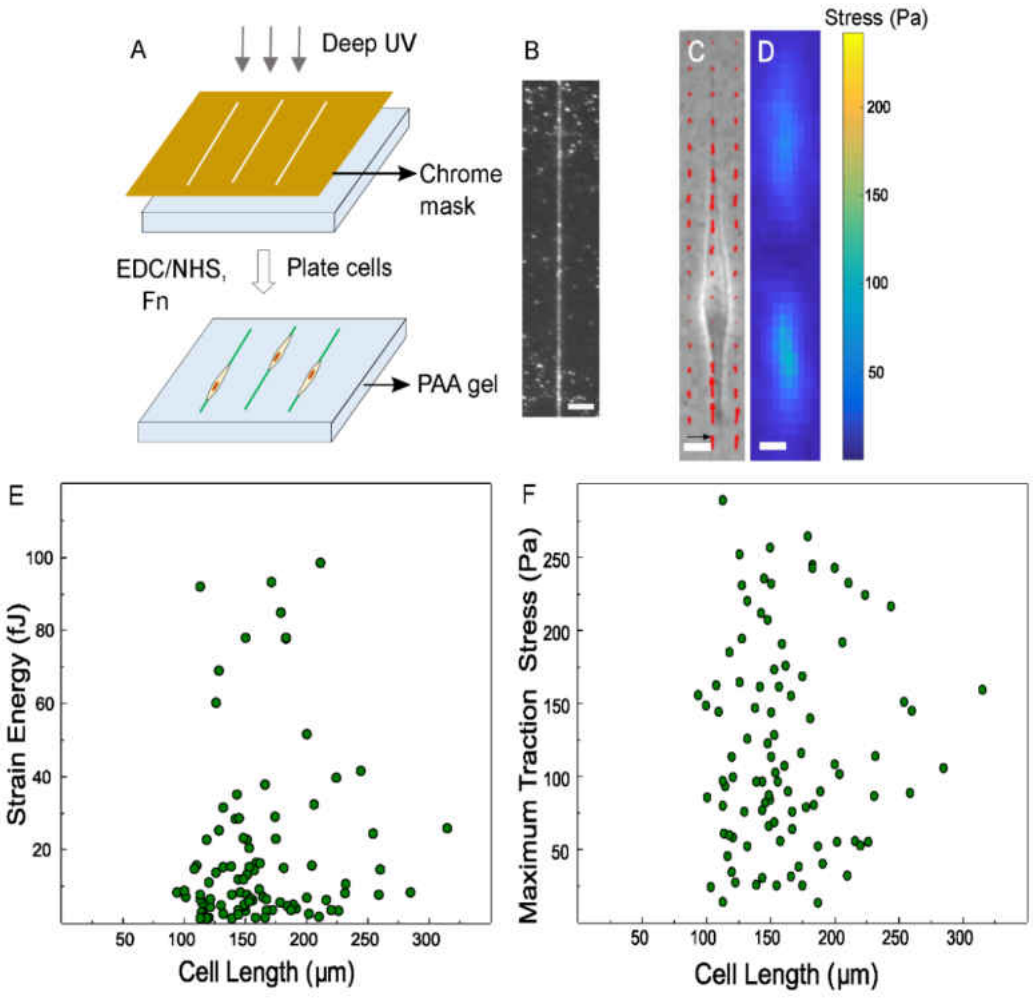


Figure 5. Fibrillar force exertion is not correlated with cell length. (A) Schematic depiction of the method used to micro-pattern 1.5 μm fibronectin lines on a polyacrylamide (PAA) gel using deep UV illumination of the PAA gel through a chrome-coated quartz photomask, followed by incubation with EDC/sulfo-NHS and fibronectin (Fn). The plated cells adhere to the fibronectin lines and adopt a fibrillar morphology. (B) Fluorescence image of the micropatterned line as revealed by fibronectin doped with fluorescent fibrinogen. (C) Phase image of an NIH 3T3 cell on a 1.5 μm fibronectin line on a 45 kPa PAA gel superimposed with traction stress vectors (red). Scale bar for traction vectors (black arrow) is 100 Pa. (D)

Heat map representation of the traction stress exerted. Traction stress heat map color scale is shown on the right. Scale bar in (B-D) is 20 μm. (E) Scatter plot of the strain energy (in fJ) associated with traction force exertion versus cell length (in μm), data from 97 cells. (F) Scatter plot of the maximum traction stress exerted (in Pa) versus cell length (in μm).

In order to assess the role of micro-environmental stiffness in fibrillar cell force exertion, we micropatterned fibronectin lines on PAA gels of stiffness 13 and 45 kPa, within a range of stiffness at which the traction force for 3T3 cells varies with stiffness in 2D [52, 75]. The difference in cell lengths corresponding to these substrate stiffnesses was statistically significant but <15% (Figure 6A). As shown by the traction heat maps in Figure 6B,C, the traction stress exerted by fibrillar 3T3 cells was prominently localized at either cell end for both stiffnesses. Importantly, both the strain energy (Figure 6D) and the maximum traction stress (Figure 6E) of the fibrillar cells did not change significantly with stiffness ($p = 0.39$ and 0.11, respectively). This implies that fibrillar cells exert forces in a manner that is not as strongly sensitive to the microenvironmental stiffness as for 2D [52]. However, as the difference in cell lengths for these different stiffnesses is not large, one can expect the strain energy to not be affected by much if geometry (which translates to cell length here) is indeed a determinant of strain energy [52].

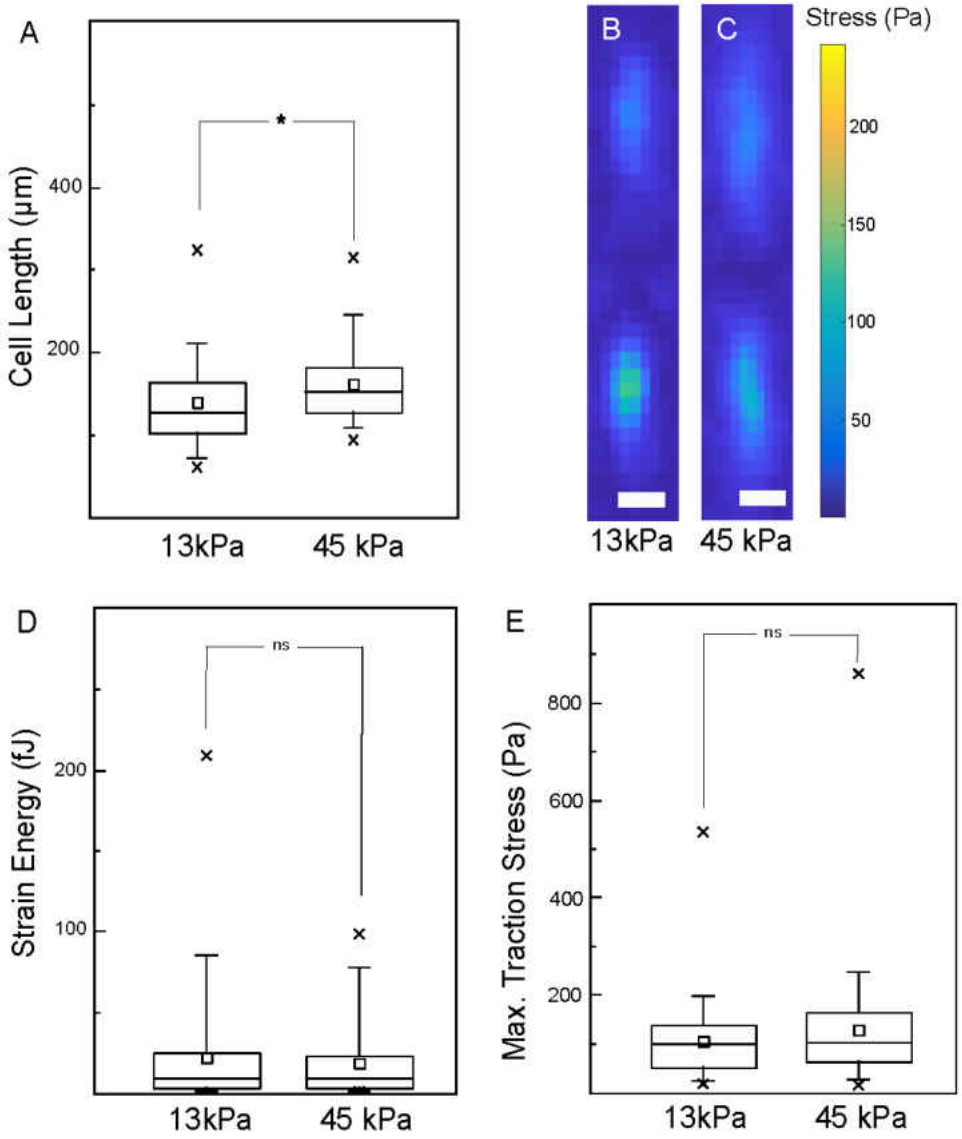


Figure 6. Fibrillar force exertion is not sensitive to substrate stiffness. (A) Box plot comparing the fibrillar cell length on fibronectin lines on 13 kPa (83 cells) and 45 kPa (97 cells) PAA substrates. (B-C) Heat map representation of the traction stress exerted for substrate Young's moduli of 13 kPa (B) and 45kPa (C). The scale bars for distance is 20 µm. Traction stress heat map color scale is shown on the right. (D, E) Box plots comparing the strain energy (D) and the maximum traction stress (E) exerted by cells adherent on

fibronectin lines on substrates of Young's moduli 13 kPa and 45kPa. In the box plots, the small square represents the mean, the horizontal line represents the median, cross (x) represents minimum or maximum value, lower and upper sides of the large box represent the 25 and 75 percentile values and whiskers represent the 5 and 95 percentile values.

We then wanted to determine as to what factors influence the level of forces exerted by fibroblasts in a fibrillar geometry. Immunofluorescence staining of the actin cytoskeleton showed that the cells displayed prominent linear actin bundles along the length of the cell, anchored at either end of the cell (Figure 9A). We therefore tested if inhibiting formin, which is a family of linear actin nucleators, would impact the actin cytoskeleton and thereby possibly affect cell force exertion. Accordingly, treatment of fibrillar cells with 20 μM SMIFH2, a pan-formin inhibitor, decreased actin localization to the ends of the cell (Figure 9B,C). Formin inhibition also reduced the fibrillar cell length by 25% (Figure 7A). Importantly, traction force measurements showed that formin inhibition reduced the strain energy and the maximum exerted traction stress by 46 and 35%, respectively (Figure 7B-E) - effects similar to that found in 2D [34].

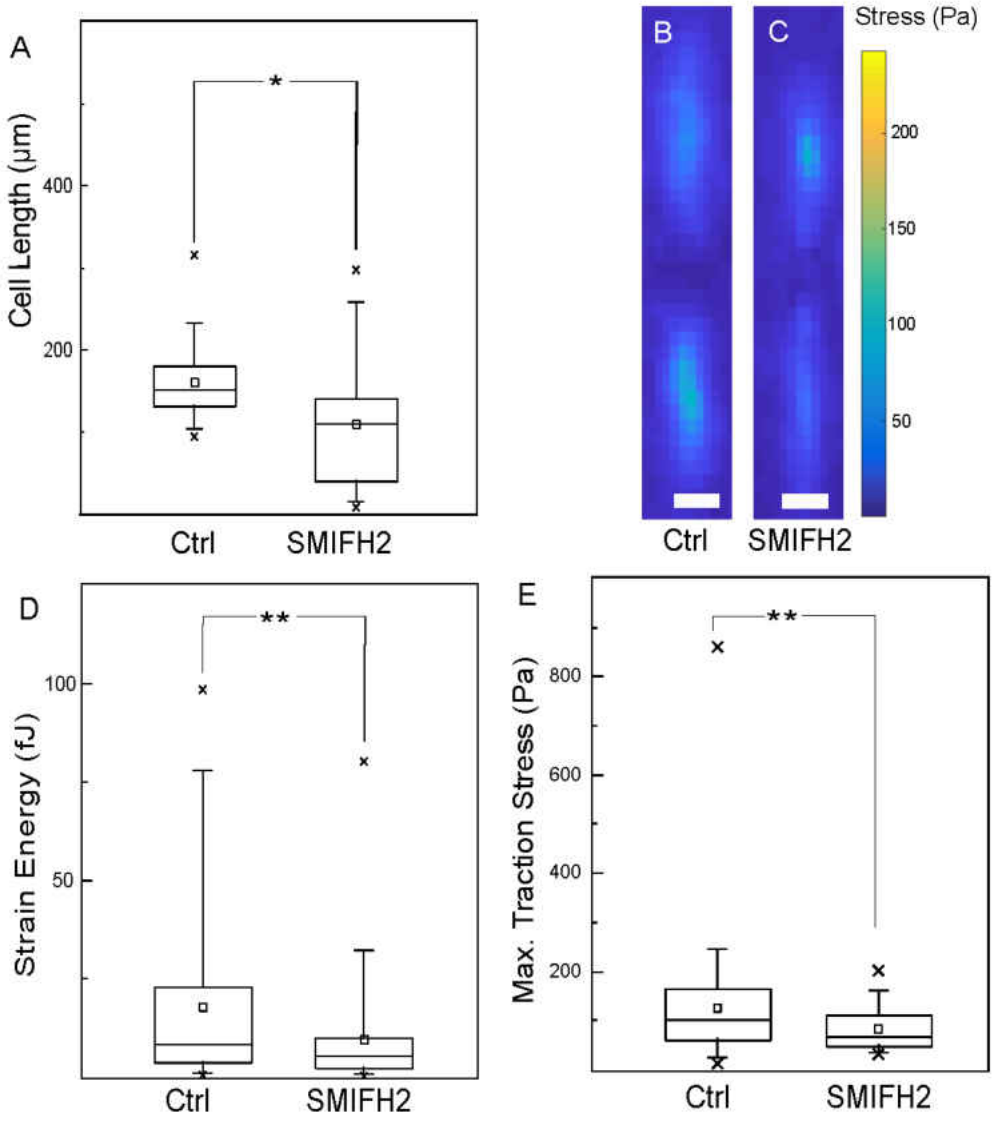


Figure 7. Effect of formin inhibition on fibrillar force exertion. (A) Box plot comparing the fibrillar cell length on fibronectin lines for control (97 cells) and 20 µM SMIFH2-treated (57 cells) cells on 45 kPa PAA substrates. (B-C) Heat map representation of the traction stress exerted by control and SMIFH2-treated cells. The scale bars for distance is 20 µm. Traction stress heat map color scale is shown on the right. (D, E) Box plots comparing the strain energy (D) and the maximum traction stress (E) exerted by control and SMIFH2-treated cells. In the box plots, the small square represents the mean, the horizontal line

represents the median, cross (x) represents minimum or maximum value, lower and upper sides of the large box represent the 25 and 75 percentile values and whiskers represent the 5 and 95 percentile values.

Finally, we wanted to assess whether reducing the level of traction forces exerted by the cells adversely impacted fibrillar cell migration. We therefore measured the fibrillar cell migration speeds of control cells as well as those treated with the formin inhibitor SMIFH2 (Figure 8A,B). Contrary to what was found in suspended fibers [62], formin inhibition did not significantly alter the average fibrillar cell migration speed ($p = 0.89$, Figure 8C). Thus, fibrillar cell migration speed was not correlated to the level of fibrillar force exertion. This result is similar to what was obtained for untreated epithelial cells on wider lines, albeit specifically for only the more elongated cells [73]. The difference in results between our experimental model and that from studies using suspended fibrils may be due to the following reasons [59, 62]: our model captures the overall micro-environmental stiffness of tissues, which is in the kPa range. Suspended fibers (made of polymers such as polystyrene) have stiffness in the GPa range [59], similar to that of individual collagen fibrils [76]. In fact, average cell migration rates were about a factor of two to three lower in our system compared to suspended fibrils [62] or micro-patterned lines on glass [4]. Fibrillar cells *in vivo* may be expected to mechanically interact with both the local stiff fibril as well as the softer extended micro-environment. Greater knowledge of forces exerted by cells in fibrillar contexts [77] and their reciprocal relationship with micro-environmental stiffness can be expected to continue to advance our understanding of disease states such as cancer and fibrosis.

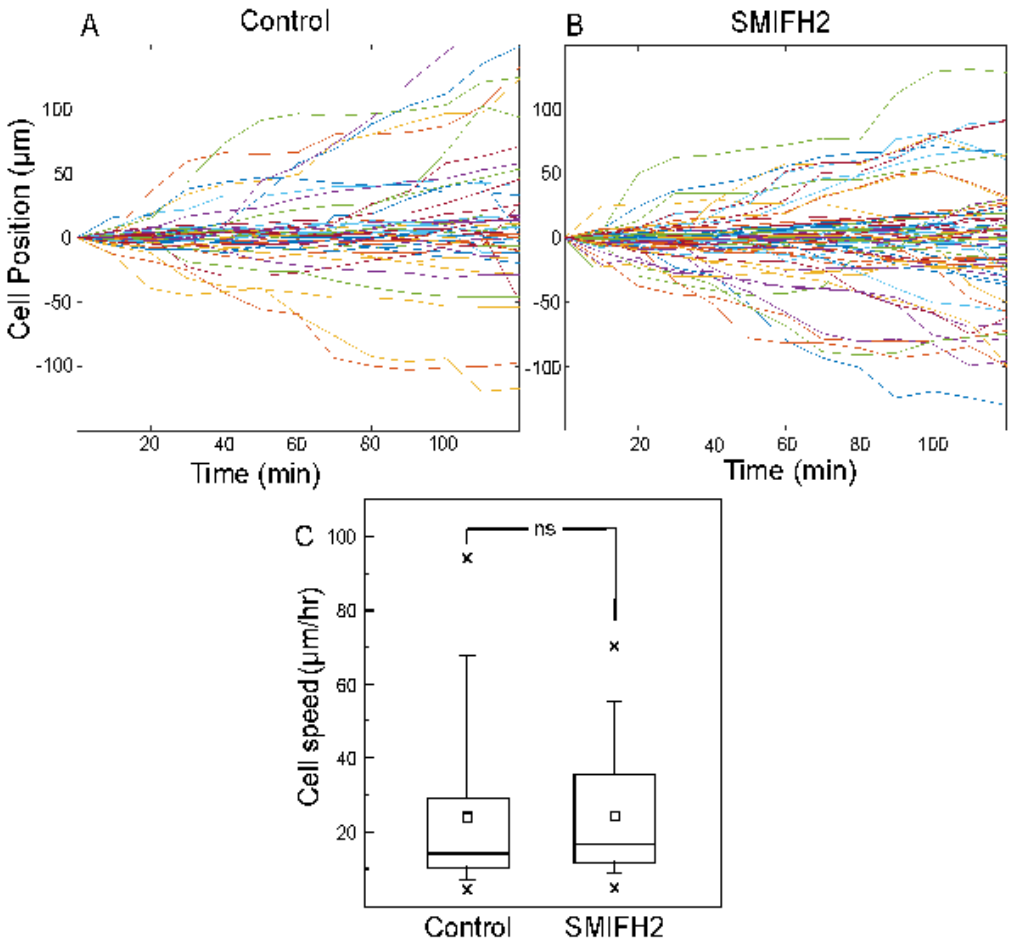


Figure 8. Fibrillar cell migration speed is not affected by formin inhibition. (A, B) Cell position is plotted as a function of time over 2 hours for (A) control (56 cells) and (B) SMIFH2 treated (77 cells) 3T3 cells. Cells were on 1.5 µm fibronectin lines on 45 kPa PAA gels for both cases. (C) Box plots comparing the fibrillar cell migration speed for control versus SMIFH2-treated cells. In the box plots, the small square represents the mean, the horizontal line represents the median, cross (x) represents minimum or maximum value, lower and upper sides of the large box represent the 25 and 75 percentile values and whiskers represent the 5 and 95 percentile values.

**Acknowledgments**

We thank Margaret Gardel for allowing generous use of the rheometer. We thank Benedikt Sabass and Ulrich Schwarz for the force reconstruction scripts.

**Funding**

This work was supported by the Thomas F. and Kate Miller Jeffress Memorial Trust. The funding source had no role in study design; in the collection, analysis and interpretation of data; in the writing of the report; or in the decision to submit the article for publication.

**2.4 Supporting information**

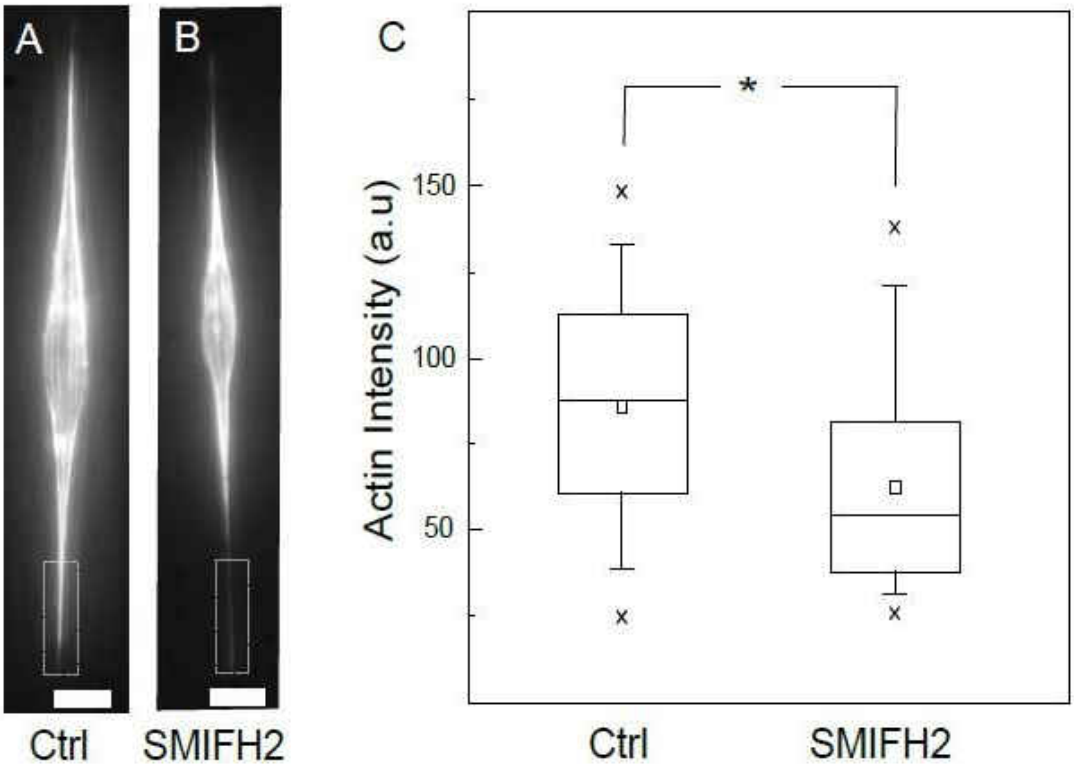


Figure 9. Formin inhibition decreases actin localization to fibrillar cell ends. (A, B) Immunofluorescence images of NIH 3T3 cells on fibronectin lines on 45 kPa PAA substrates, either untreated (control) (A) or treated with 20 μM SMIFH2 (B). The scale bars for distance is 20 μm. (C) Box plot of the average actin intensity at the ends of

fibrillar cells (20% of cell length), as indicated by the dotted boxes in (A,B), for control (16 cells) and SMIFH2-treated (20 cells) cells. In the box plots, the small square represents the mean, the horizontal line represents the median, cross (x) represents minimum or maximum value, lower and upper sides of the large box represent the 25 and 75 percentile values and whiskers represent the 5 and 95 percentile values.

# CHAPTER 3

# DEVELOPMENT OF A BIOMIMETIC E-CADHERIN SUBSTRATE WITH CELL-LIKE STIFFNESS

## 3.1 Introduction

Cell-cell adhesion is required to maintain tissue integrity and functionality. Epithelial cells interact with their external microenvironment through both cell-ECM interactions using integrin receptors as well as cell-cell interactions through E-cadherin receptors. Both these interactions are highly dependent on cell-generated forces. Previous studies showed that cell-cell endogenous forces are correlated with cell-ECM forces [48] and the crosstalk between E-cadherin and integrin mediated adhesions have also been investigated [78].

Earlier studies have used E-cadherin coated glass surfaces to restrict the cell's adhesive interactions to E-cadherin binding, in order to identify the role of E-cadherin adhesion in "outside-in" signaling [79-81]. It was found that E-cadherin adhesion formation requires actomyosin activity through activation of Rho family GTPases. In particular, by implementing the E-cadherin coated surface platform, it was found that E-cadherin formation in HEK 293 cells requires actomyosin activity as well as actin nucleation through constituent proteins [82]. Moreover, it was found that the Arp2/3 complex promotes nascent E-cadherin adhesion formation in CHO cells [81]. On the other hand, formin is required for cell spreading and the formation of robust E-cadherin adhesions at leading edges [46]. When E-cadherin adhesions undergo homophilic binding, PI 3-kinase promotes nascent E-cadherin adhesion formation in the lamellipodia [80, 83].

Glass substrates are very rigid (with elastic modulus of the order of GPa) and their stiffness is thus way beyond that of the tissue microenvironment. Therefore, substrates with stiffness correspond to the ranges of tissue stiffness in vivo are required to characterize the possible mechano-responsive behavior of epithelial cells in a microenvironment of cell-like stiffness. The stiffness of epithelial cells can vary within a wide range, depending on factors such as their normal or cancerous state (Figure 10). Using the atomic force microscopy (AFM) technique to probe cell stiffness, it has been found that cancerous epithelial cells are softer than non-tumorigenic epithelial cells [27]. Moreover, non-tumorigenic human kidney cells were found to be less deformable than cancerous cells. Also, highly invasive ovarian cancer cells were found to be softer than the cells exhibiting less invasive phenotypes [84, 85]. Regardless of cancer type (bladder, colon, melanoma, prostate, and breast), single cancerous cells were found to be more deformable than single normal cells [86, 87]. Moreover, the cell microenvironment also influences cell stiffness. For instance, in a monolayer normal epithelial cells, the cells inside the monolayer are stiffer than peripheral cells [88]. In general, the main factor that contributes to cell stiffness is cytoskeleton. For instance, older human epithelial cells are stiffer than younger cells due to the presence of a higher density of cytoskeleton such as microtubules, actin and intermediate filaments [24]. The cytoskeleton also contributes to cell stiffness during cell division, in which, the formation of a contractile ring and furrow makes the cells stiffer [25]. In addition to the effect of the cytoskeleton, cell adhesion molecules play a key role in influencing cell stiffness. It was reported that cancerous epithelial cells become softer and less adhesive due to the loss of E-cadherin adhesion [89, 90].

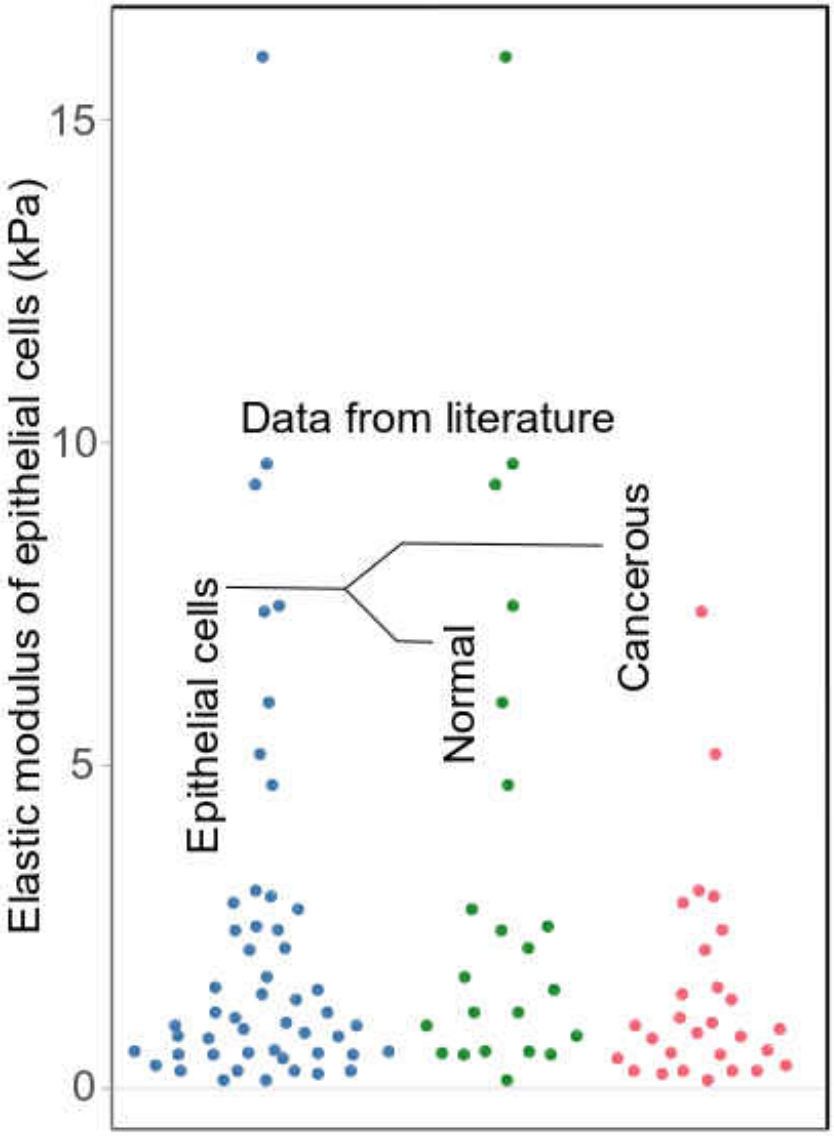


Figure 10. Scatter plot of epithelial cell stiffness values. Elastic modulus of epithelial cells are shown in blue circles, and further split into normal cells and cancerous cells, shown in green and red respectively.

## 3.2 Methods

### 3.2.1 Cell culture

C2bbe cells were grown under 5 % $CO_2$ at 37 degrees C in Dulbecco's modified Eagle's medium with 1 % L-glutamine and 1 % penicillin for serum starved samples, but with 10 % fetal bovine serum otherwise. Before each experiment, cells were detached from cell culture petri-dishes using a EDTA based cell dissociation reagent (Versene). The cells were seeded on samples, then incubated in DMEM (with or without serum) for 2 hours at 37 C.

### 3.2.2 Preparation of direct E-cadherin-Fc coated glass

To prepare the E-cadherin-Fc coated glass surface, a 22 x 22 mm coverslip was exposed to deep UV for 10 minutes. Then the hydrophilic glass was incubated with 20 µl of 0.1 mg/ml recombinant E-cadherin-Fc (Sinobiological) for 2 hours. Afterwards, the E-cadherin-Fc coated glass was washed with DPBS (with Ca / Mg) 3 times for 5 minutes each time.

### 3.2.3 Preparation of oriented, immobilized E-cadherin-Fc coated glass

For the oriented immobilization of E-cadherin-Fc coated on a glass surface, a 22 x 22 mm coverslip was incubated with 40 µl of protein-A (pA) for 1 hour (Figure 11A). After several washing steps with DPBS (with Ca / Mg), the pA coated glass was incubated with 20 µl of 0.1 mg/ml recombinant E-cadherin-Fc for 2 hours (Figure 11B). Afterwards, the glass was washed with DPBS (with Ca / Mg) 3 times for 5 minutes each time. Then, the

sample was incubated with 20 µl of 1 mg/ml Fc fragment for 1 hour (Figure 11C) followed by washing with DPBS (with Ca / Mg).

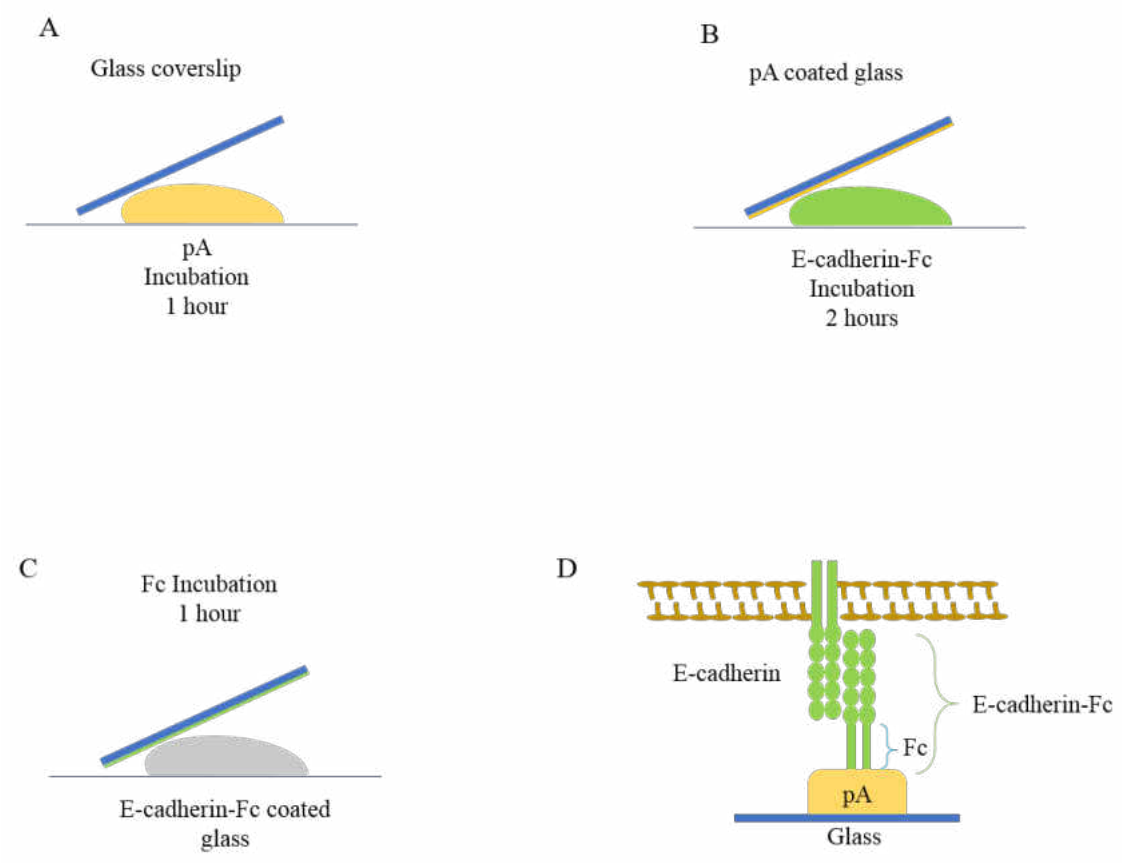


Figure 11. Schematic representation of oriented immobilization of E-cadherin-Fc on a protein-A coated glass. (A) protein-A incubation for 1 hour, (B) E-cadherin-Fc incubation for 2 hours and (C) Fc coating for 1 hour. (D) Schematic configuration of biomimetic E-cadherin surface.

### 3.2.4 Preparation of oriented immobilization of E-cadherin-Fc coated soft-silicones

For the oriented immobilization of E-cadherin-Fc on cured soft silicones, the sample was exposed to shallow UV (~305 nm UV) for 5 minutes (Figure 12A) followed by 1 mg/ml of protein-A using EDC NHS chemistry for 1 hour (Figure 12B). After several washing

steps with DPBS (with Ca / Mg), the pA coated sample was incubated with 20 µl of 0.1 mg/ml recombinant E-cadherin-Fc for 2 hours (Figure 12C). Afterwards, the sample was washed with DPBS (with Ca / Mg) 3 times for 5 minutes each time. Then, the sample was incubated with 20 µl of 1 mg/ml Fc fragment for 1 hour (Figure 12D) followed by washing with DPBS (with Ca / Mg).

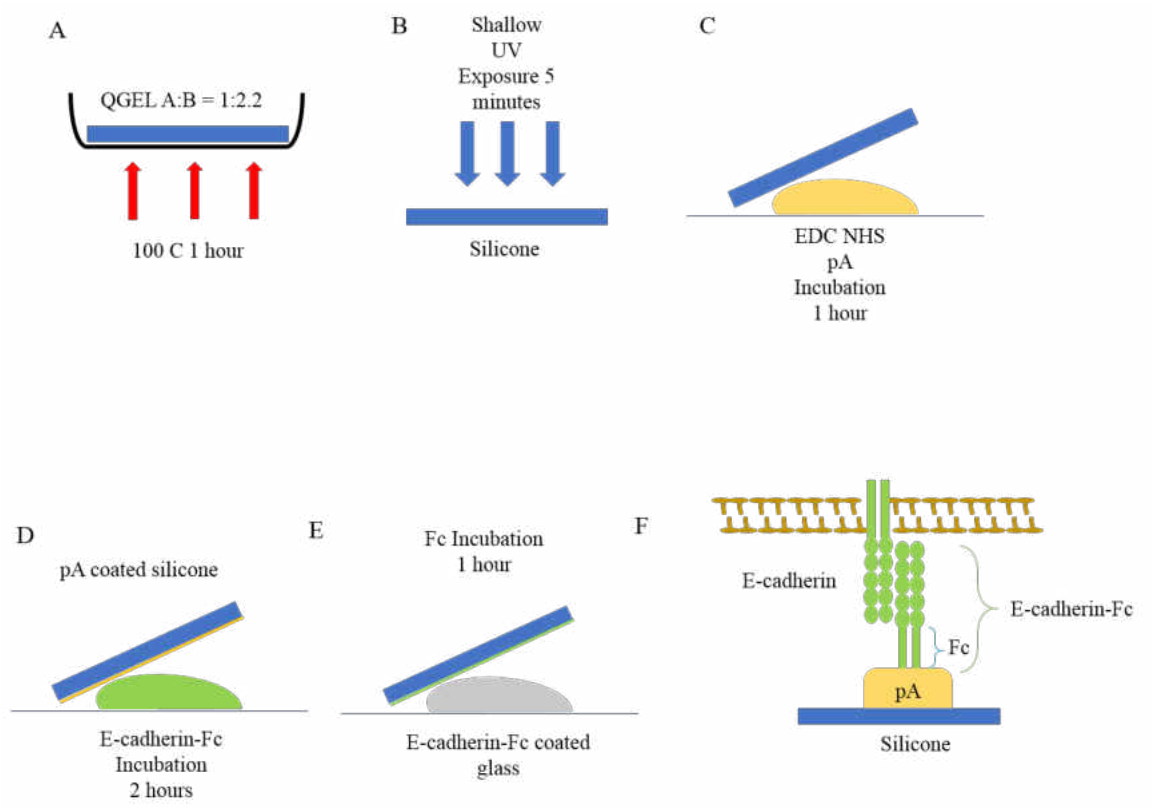


Figure 12. Schematic representation of oriented immobilization of E-cadherin-Fc on QGEL300 silicone. (A) Curing the mixture on a hot plate at 100 C for 1 hour, (B) shallow UV exposure for 5 minutes, (C) protein-A EDC NHS incubation for 1 hour, (D) E-cadherin-Fc incubation for 2 hours and (E) Fc coating for 1 hour and (F) the schematic configuration of the biomimetic E-cadherin surface is shown.

### 3.2.5 Immunostaining

Fixed cells were imaged using a Leica DMi8 epifluorescence microscope (Leica Microsystems, Buffalo Grove, IL) equipped with 10, 20 and 40 × objectives and a Clara cooled CCD camera (Andor Technology, Belfast, UK). Cells were fixed with 4% paraformaldehyde (Electron Microscopy Sciences, Hatfield, PA), with 1.5% Bovine Serum Albumin and 0.5% Triton. Alexa-488 conjugated phalloidin was from Thermo Fisher Scientific. Mouse anti β-catenin and rabbit anti paxillin antibodies were from BD Biosciences and Abcam respectively.

## 3.3 Results and Discussion

### 3.3.1 Cells form undesirable focal adhesions also on E-cadherin-Fc-coated glass

C2bbe epithelial cells bind to neighboring cells primarily via E-cadherin adhesions to form cell-cell contacts. Therefore, we wanted to assess the E-cadherin adhesion of single C2bbe cells on a glass coated with E-cadherin-Fc. We prepared a direct E-cadherin-Fc coated glass as explained in section 3.2.2 then plated C2bbe cells on them and waited for 2 hours. To determine the localization of E-cadherin adhesion on this direct E-cadherin-Fc coated glass, we used immunofluorescence staining of β-catenin (Figure 13A). To make sure that C2bbe cells adhered to E-cadherin-Fc and did not bind to ECM, we also checked the focal adhesion localization. Thus, we imaged paxillin, an adaptor protein which is localized at focal adhesion (indicative of the cell adhering to ECM). It was evident that focal adhesions formed on direct E-cadherin-Fc coated glass (Figure 13B). Actin connected to both focal adhesions and “dot-like” E-cadherin adhesions (Figure 13C). Therefore, with this system, it is difficult to separate cell response to the micro-

environment via focal adhesions and E-cadherin adhesions. It was previously shown that mouse myogenic C2 cell, expressing N-cadherin, forms cadherin adhesions in absence of serum [83]. This condition avoided any contribution from other adhesion molecules. Thereby, in order to better characterize cell response due to E-cadherin adhesion, we seeded C2bbe cells on a direct E-cadherin-Fc coated glass in serum-free medium conditions. Then, we used immunofluorescence staining of β-catenin (Figure 14A) and paxillin (Figure 14B). The results suggested that, in absence of serum, we can avoid focal adhesion formation and allow only E-cadherin adhesion. Figure 14C also shows the corresponding actin staining.

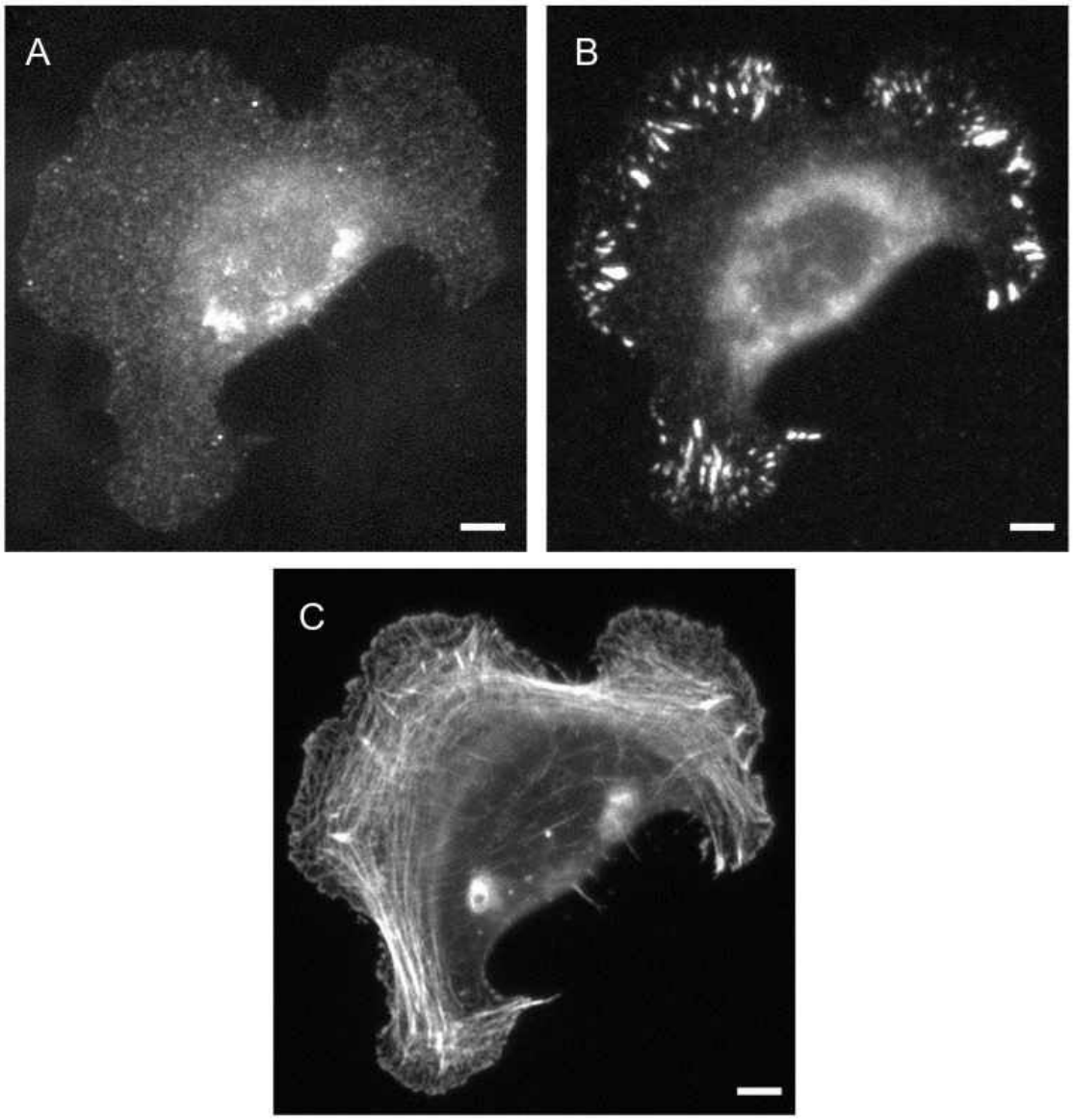


Figure 13. Formation of undesirable focal adhesions on direct E-cadherin-Fc coated glass. Immunofluorescence images of C2bbe cells plated E-cadherin-Fc coated glass, stained for (A) β-catenin, (B) paxillin and (C) actin. (Scale bar: 5 μm)

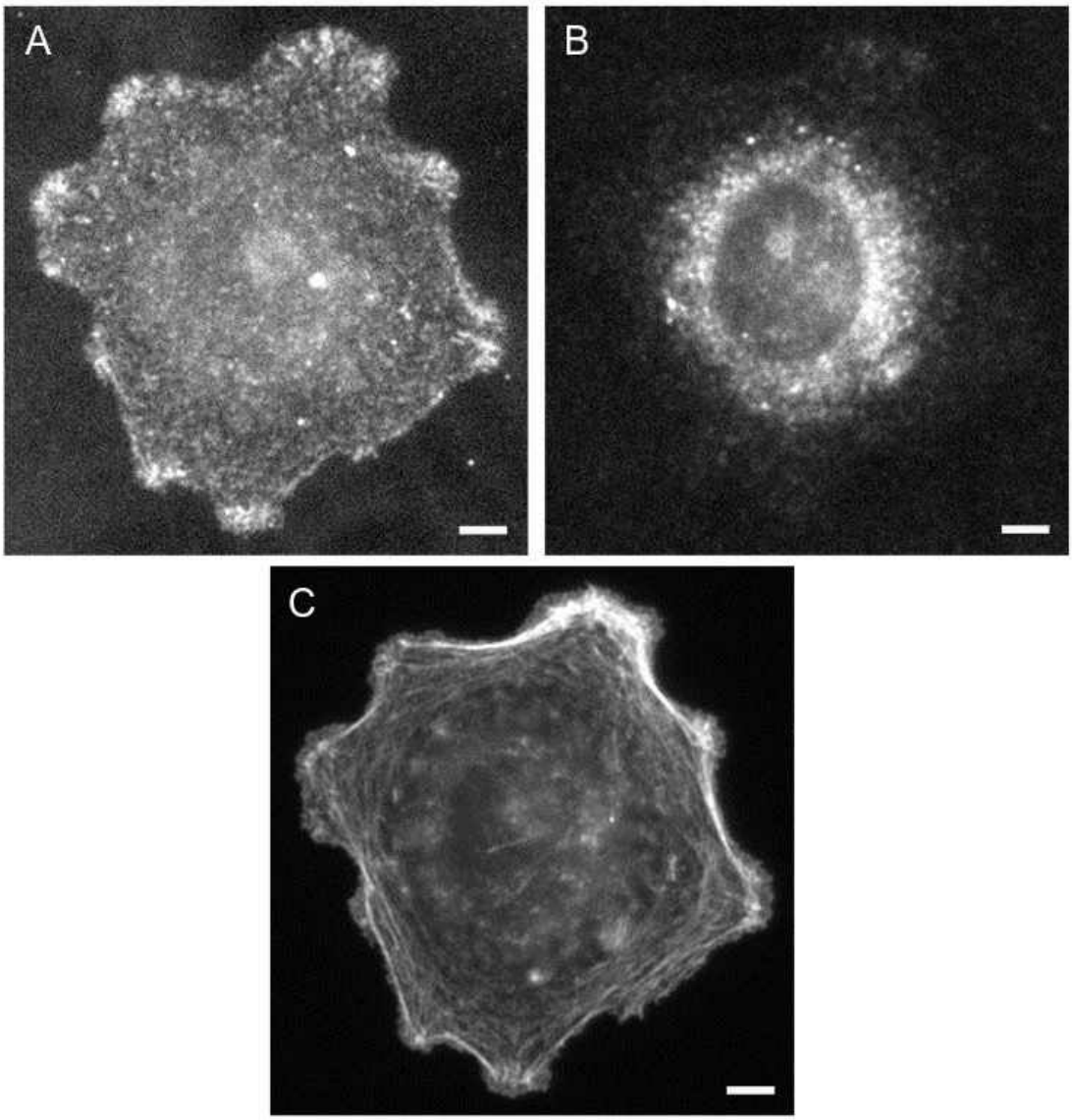


Figure 14. Direct E-cadherin-Fc coated glass in serum-free medium.

Immunofluorescence images of C2bbe cells plated E-cadherin-Fc coated glass, stained for (A) β-catenin, (B) paxillin and (C) actin. (Scale bar: 5 μm)

### 3.3.2 Oriented immobilization of E-cadherin-Fc on glass

In addition to the direct E-cadherin-Fc coated method, we implemented oriented immobilization of E-cadherin-Fc. In an oriented, immobilized E-cadherin-Fc coated

substrate, the surface is initially coated with protein A. Protein A has a strong affinity to immunoglobulin (IgG) Fc [91]. This way, E-cadherin-Fc binds at its N-terminus to the N-terminus of cellular E-cadherin [92]. Therefore, we seeded C2bbe cells on oriented immobilized E-cadherin-Fc coated glass. We observed that, similar to direct E-cadherin-Fc coated glass, not only E-cadherin adhesions, but also focal adhesions formed in the presence of serum (Figure 15A-B). Furthermore, actin bundles were mainly localized with focal adhesions (Figure 15C).

In order to avoid focal adhesions, we used serum-free conditions along with the oriented immobilization of E-cadherin on glass. Immunofluorescence images show that, in the absence of serum, E-cadherin adhesions marked by are larger rather than dot-like(Figure 16A). In addition, paxillin was not present in the absence of serum (Figure 16B) and actin filaments are mainly connected to E-cadherin adhesions. In the presence of serum, cells on either direct E-cadherin-Fc coated glass or oriented, immobilized E-cadherin-Fc on glass exhibit paxillin localization in focal adhesions in all cells. Thus, oriented E-cadherin-Fc surfaces using serum-free condition provides a viable platform for studying E-cadherin adhesion-specific effects.

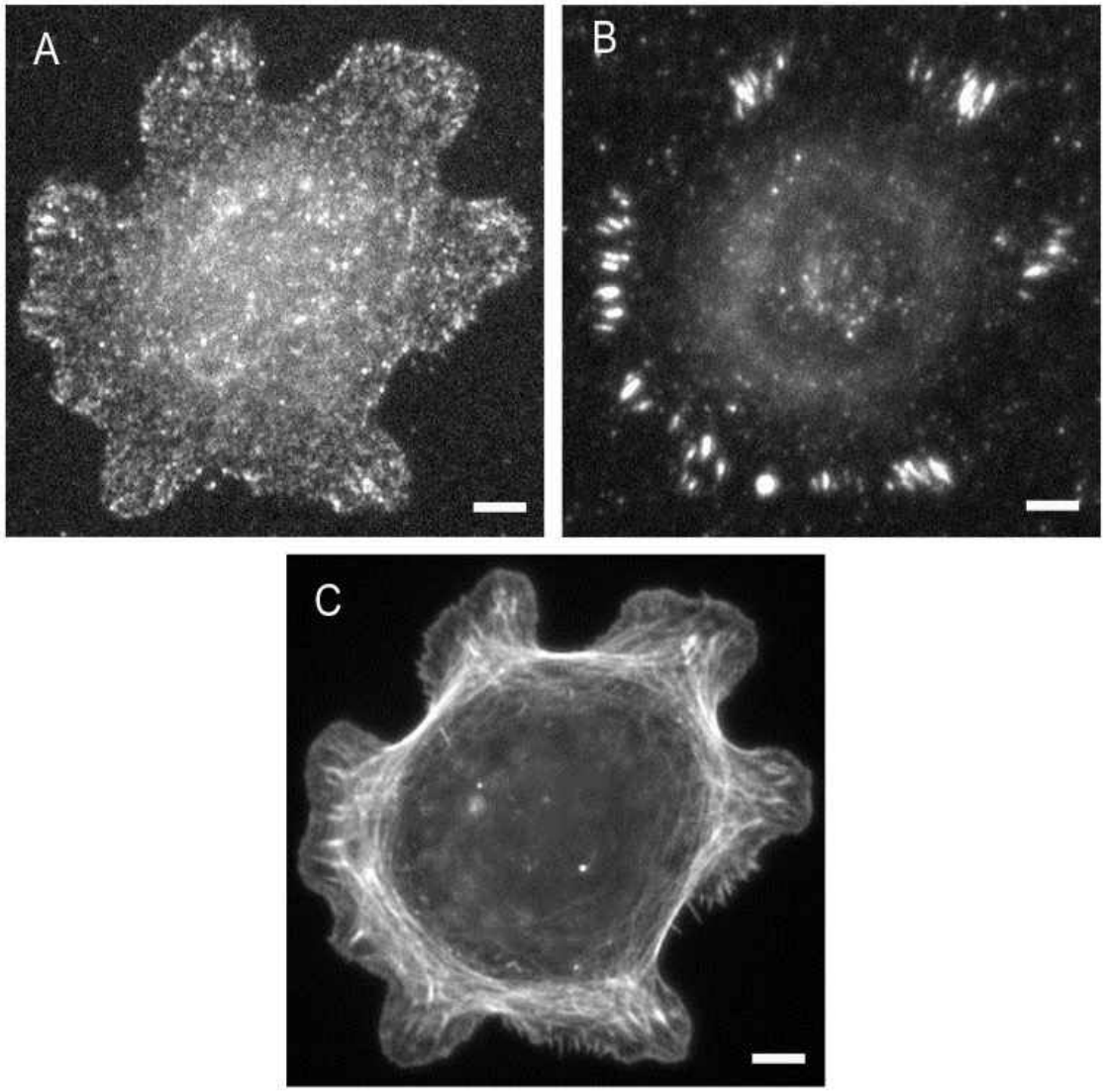


Figure 15. Formation of undesirable focal adhesions on oriented, immobilized E-cadherin-Fc on glass. Immunofluorescence images of C2bbe cells plated on oriented protein-A / E-cadherin-Fc/ Fc coated glass, stained for (A) β-catenin, (B) paxillin and (C) actin. (Scale bar: 5 μm)

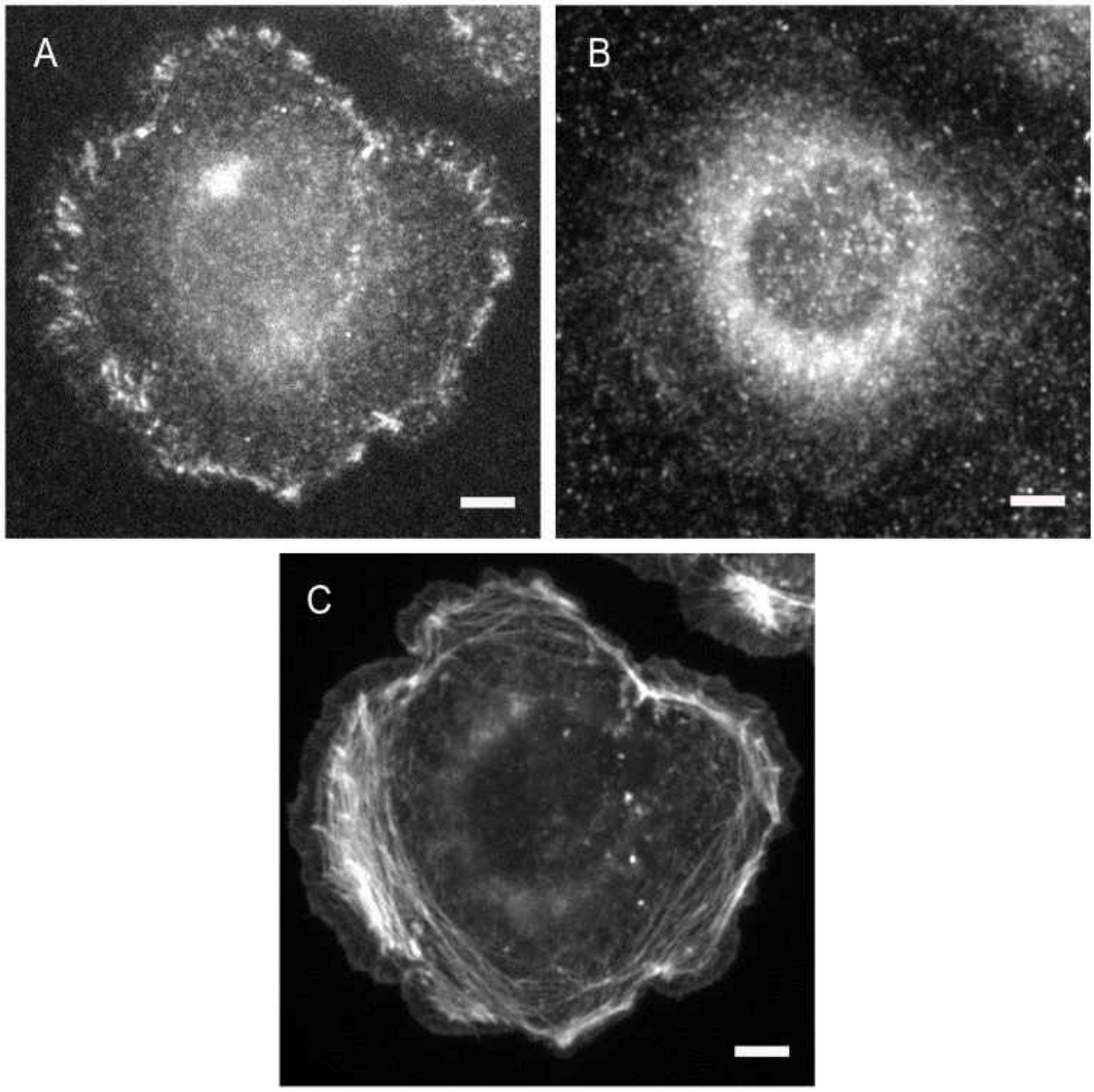


Figure 16. Oriented immobilization of E-cadherin-Fc on glass in serum-free medium. Immunofluorescence images of C2bbe cells plated on oriented protein-A / E-cadherin-Fc/ Fc coated glass, stained for (A) β-catenin, (B) paxillin, and (C) actin. (Scale bar: 5 μm)

### 3.3.3 Soft silicones as possible substrates and their rheological properties

Cell adhesion is regulated by physical cues such as substrate rigidity [13, 20]. It has been found that cells respond to the stiffness of their microenvironment and undergo specific physiological changes [12]. The stiffness of epithelial cells varies widely, as discussed in

the Introduction. Similar to PAA gels, soft silicones can have tunable elasticity over a physiological range. Thus, we used soft silicone substrates, whose mechanical properties were then tuned to match the targeted stiffness values in Figure 10.

In order to characterize the mechanical properties of the candidate soft silicones, we used rheology. Oscillatory rheology is an experimental technique to characterize the mechanical behavior of soft materials. By implementing this technique, we can decouple the viscous and elastic response of viscoelastic materials. The viscoelastic behavior of the polymer at ω (frequency) is characterized by the storage modulus, G′(ω), and loss modulus, G″(ω), which represent the "solid-like" and "fluid-like" behavior of a material in response to stress. For a viscoelastic material, the stress response σ on the time scale t is given by:

$$\sigma(t) = \ '(\omega)\gamma_0 \sin(\omega t) + \ ''(\omega)\gamma_0 \cos(\omega t)$$

where $\gamma(t)$ is the sinusoidal applied strain deformation with amplitude $\gamma_0$. We determine G′ and G″ as a function of ω to determine how solid-like or fluid-like state the material behaves. Prior to quantifying G′ and G″ as a function of frequency, it is important to assess if the applied strain deformation is small enough remain in the linear regime. Soft materials exhibit a nonlinear stress response if they undergo large strain deformation.

Mixtures of GEL8100 (weight ratio A:B = 2:3, 2:4, 2:7) and QGEL300 (weight ratio: A:B = 1:2.2) were cured on a hot plate at 100 C for 1 hour. The CY52-276 silicone sample (weight ratio: A:B = 1:2 ) was cured on hot plate at 80C for 30 minutes. Then, a sample of each mixture with thickness of ~ 0.5 mm were mounted on the rheometer plate. Soft silicones are linear elastic isotropic incompressible materials, as long as a strain

amplitude small enough is employed, to stay in the linear regime. Therefore, an amplitude sweep test was performed for each silicone sample at constant frequency (10 rad/s) to determine the linear regime. In order to characterize the mechanical properties of the developed soft silicones, we measured the frequency-dependent storage and loss shear modulus of the samples using shear rheology with a cone and plate rheometer. We conducted the frequency sweep test at 1 % strain to quantify the shear and loss modulus as shown in Figures 17-21. We used the average of G′ values between 0.1 rad/s to 1 rad/s as this is the range most commensurate with cell contractility and relevant cytoskeletal dynamics (Table 1). Thus, we calculated the elastic modulus, E, from storage modulus, G′, by assuming that the soft silicones are isotropic and incompressible, with a Poisson ratio, υ, of 0.5: $E = 2 \times G(1 + \upsilon)$. Based on the obtained stiffness values, we considered the 0.4 kPa (GEL 8100 A:B = 2:3), 2.4 kPa (GEL 8100 A:B = 2:7), and 8.7 kPa (QGEL 300 A:B = 1:2.2) silicones as biomimetic substrates for identifying E-cadherin mechanosensitivity using C2bbe cells.

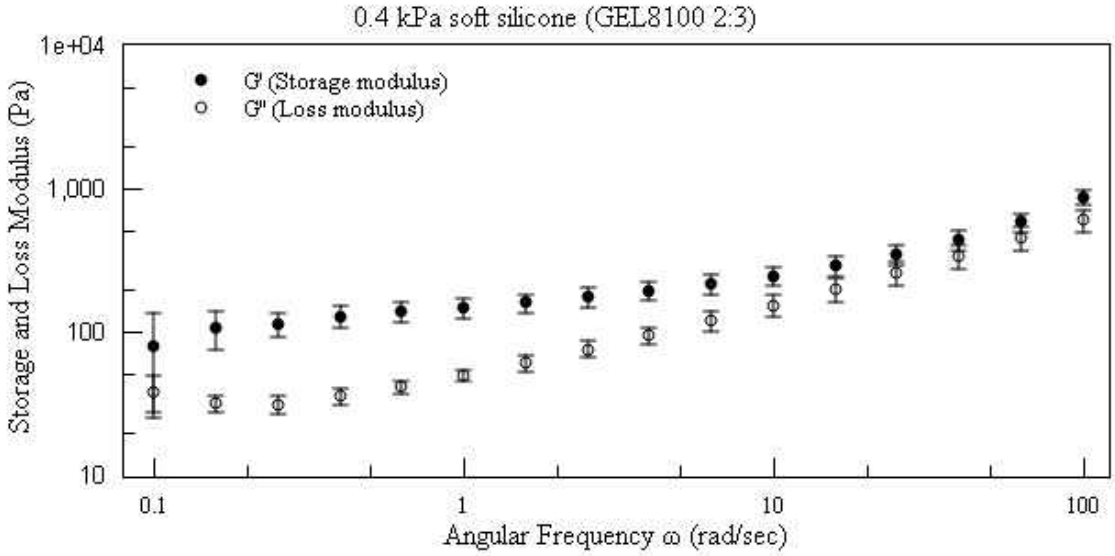


Figure 17. Mechanical characterization of 0.4 kPa silicone with frequency sweep test at 1% strain. Storage modulus (G′) and loss modulus (G″) in Pa versus angular frequency (ω) in rad/sec. Data points are mean ± SD

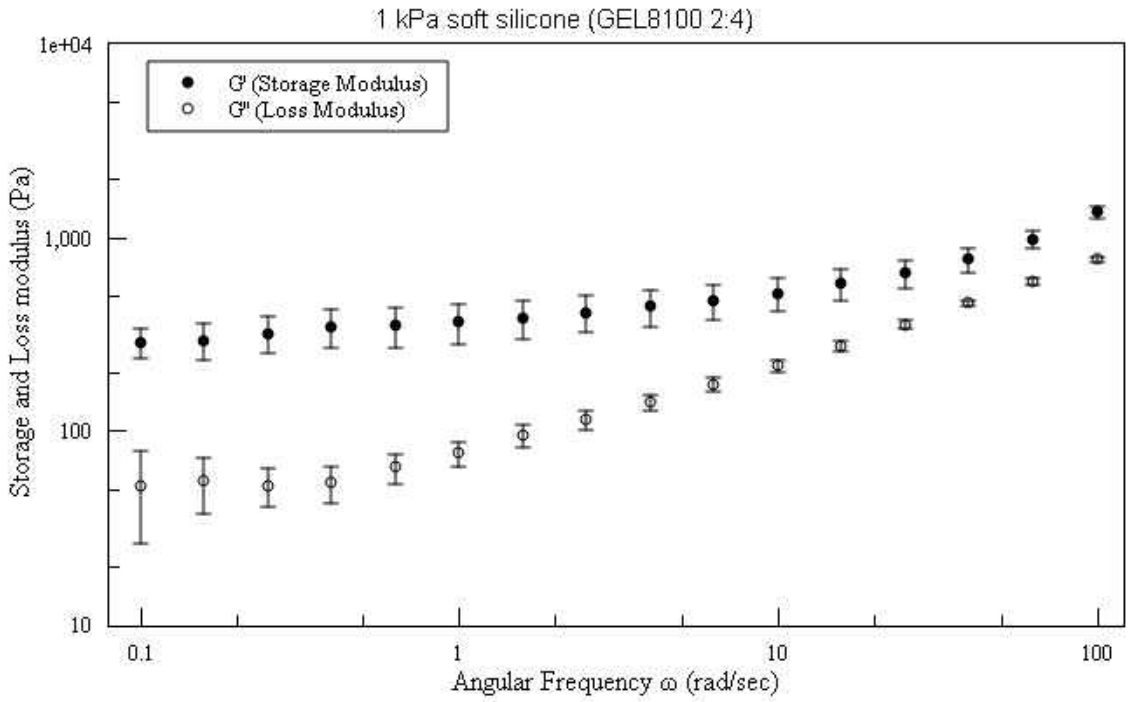


Figure 18. Mechanical characterization of 1 kPa silicone with frequency sweep test at 1% strain. Storage modulus (G′) and loss modulus (G″) in Pa versus angular frequency (ω) in rad/sec. Data points are mean ± SD

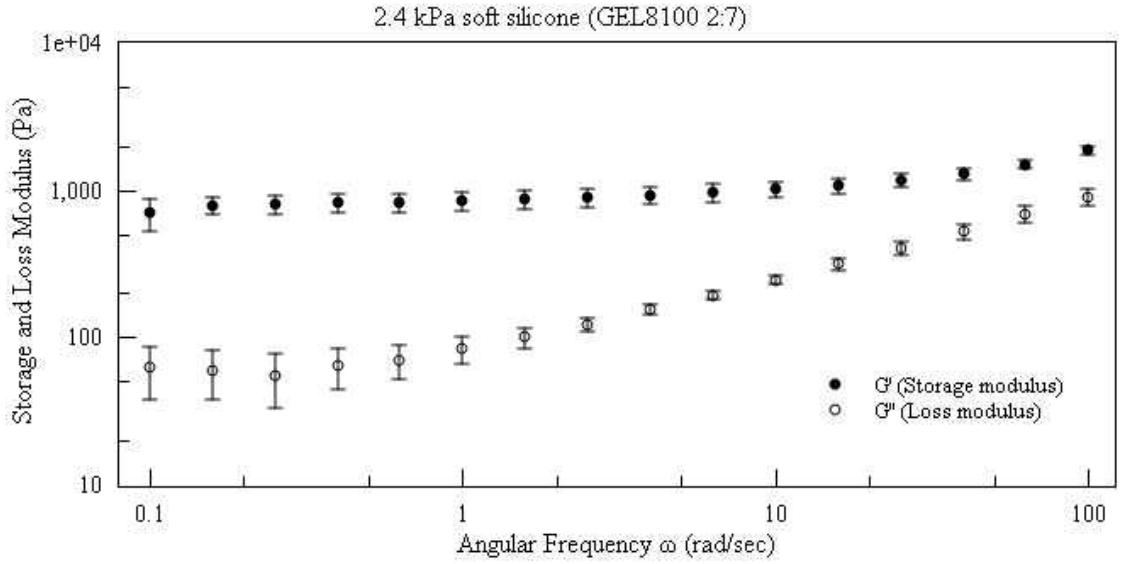


Figure 19. Mechanical characterization of 2.4 kPa silicone with frequency sweep test at 1% strain. Storage modulus (G′) and loss modulus (G″) in Pa versus angular frequency (ω) in rad/sec. Data points are mean ± SD

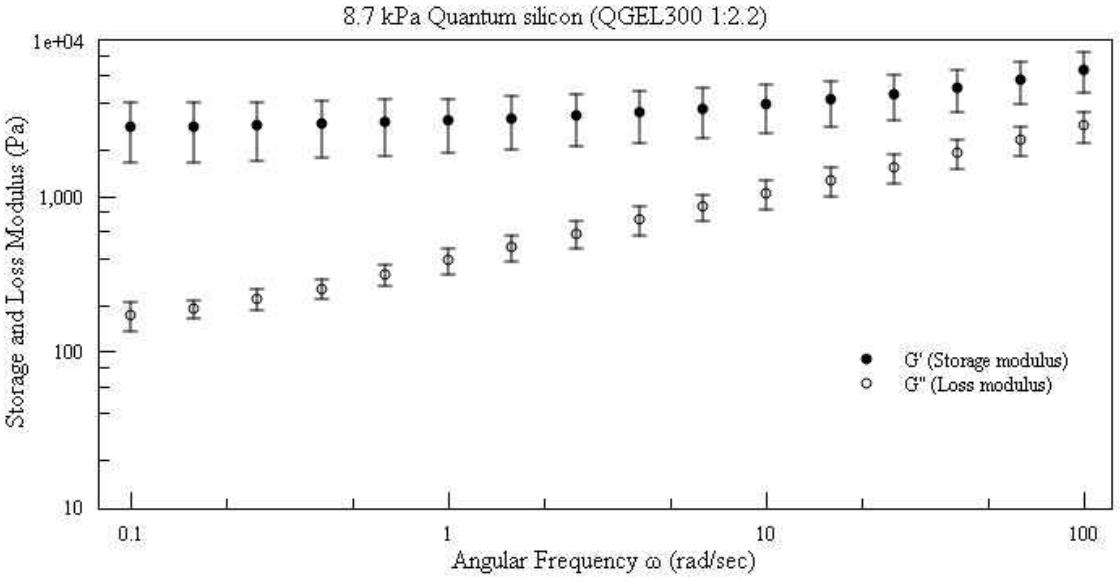


Figure 20. Mechanical characterization of 8.7 kPa silicone with frequency sweep test at 1% strain. Storage modulus (G′) and loss modulus (G″) in Pa versus angular frequency (ω) in rad/sec. Data points are mean ± SD

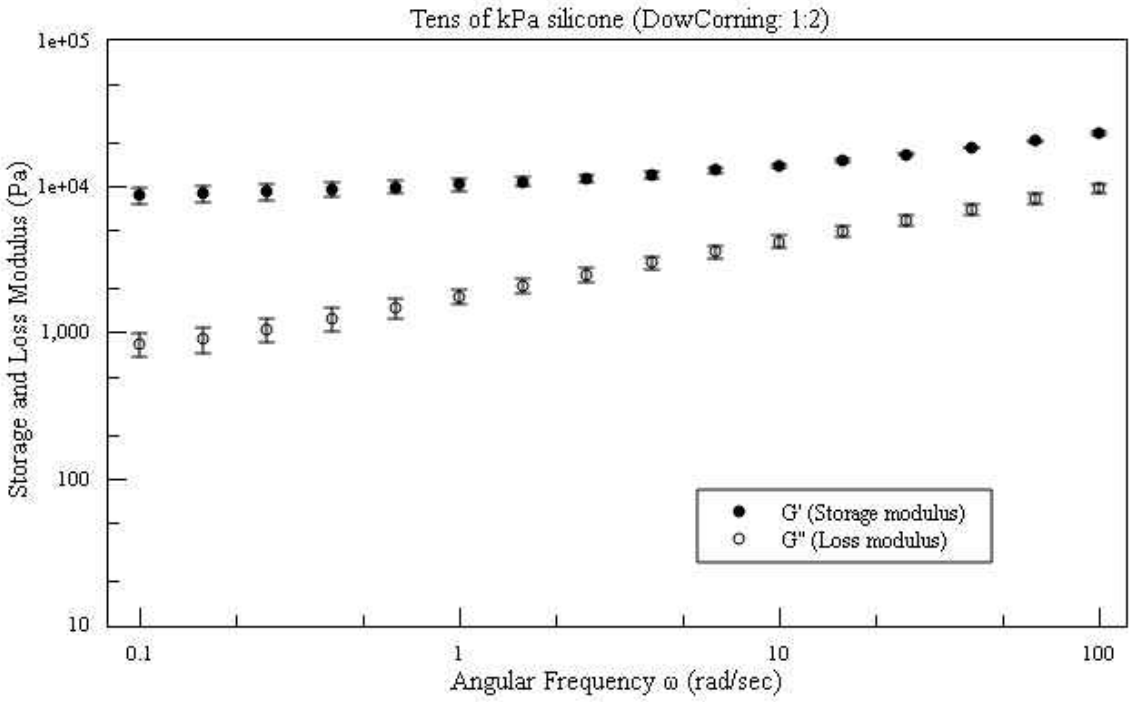


Figure 21. Mechanical characterization of tens of kPa silicone with frequency sweep test at 1% strain. Storage modulus (G′) and loss modulus (G″) in Pa versus angular frequency (ω) in rad/sec. Data points are mean ± SD. Here, 'Dow Corning 1:2' refers to Dow Corning silicone CY 52-276 A:B = 1:2.

| Silicone mixtures | (G′) Storage modulus (kPa) (mean ± SD) | (E) Elastic modulus(kPa) (mean ± SD) |
|---|---|---|
| GEL800 (A:B = 2:3) | 0.118±0.028 | 0.355±0.086 |
| GEL800 (A:B = 2:4) | 0.326±0.069 | 0.978±0.208 |
| GEL800 (A:B = 2:7) | 0.795±0.123 | 2.387±0.369 |
| QGEL300 (A:B = 1:2.2) | 2.108±0.748 | 8.739±3.508 |

| | | |
|---|---|---|
| CY 52-276 (A:B = 1:2) | 9.413±0.588 | 28.24±2.74 |

Table 1. Mechanical characterization of tunable soft silicones silicone. A table of mean ± standard deviation of shear modulus (G′) and elastic modulus (E) is shown.

### 3.3.4 Oriented immobilization of E-cadherin-Fc on soft silicone

Single C2bbe cells formed E-cadherin adhesions and avoided focal adhesions on oriented, immobilized E-cadherin on glass, in serum-free conditions. Thus, we aimed to ascertain the formation of E-cadherin adhesions on a soft silicone with similar E-cadherin presentation. We prepared oriented, immobilized E-cadherin-Fc on 8.7 kPa (QGEL A:B = 1:2.2) silicone (the stiffest substrate specified in section 3.2.4 corresponding to epithelial cell stiffness) to mimic the microenvironment of epithelial cells. Immunofluorescence image of β-catenin (Figure 22A) confirms E-cadherin adhesion presence without the formation of focal adhesions (Figure 22B) under serum free condition. It is evident that large actin bundles are connected to E-cadherin adhesions (Figure 22C).

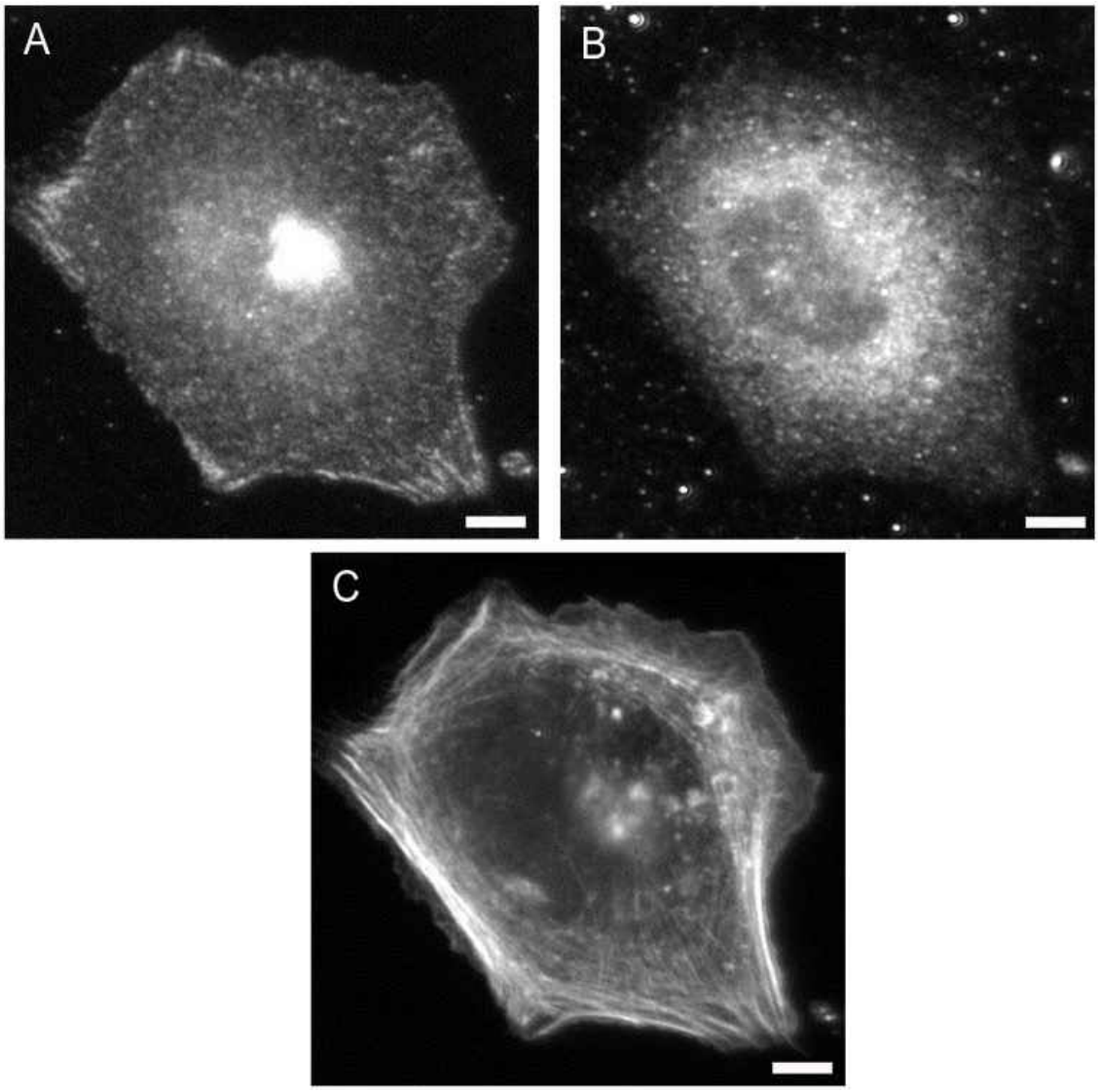


Figure 22. Oriented immobilization of E-cadherin-Fc on 8.7 kPa silicone in serum-free medium. Immunofluorescence images of C2bbe cells plated on oriented protein-A / E-cadherin-Fc/ Fc coated 8.7 kPa silicone, stained for (A) β-catenin, (B) paxillin, and (C) actin. (Scale bar: 5 μm)

# CHAPTER 4

# MODULATION OF E-CADHERIN ADHESION ON SUBSTRATES WITH CELL-LIKE STIFFNESS

## 4.1 Introduction

Epithelial cells adhere to the ECM as well as to their neighboring cells to provide tissue integrity. E-cadherin is required to maintain the cell-cell contact between epithelial cells. In addition, regulation of E-cadherin adhesion is a key factor in tissue hemostasis [44] and cell proliferation [93]. Mechanical cues such as the stiffness of the microenvironment influences cell behavior. Integrin-based rigidity sensing has been extensively investigated [12] and a few studies investigated the role of substrate rigidity in the cadherin-cadherin interaction.

Cell spreading is one of the aspects of a cell's response to substrate stiffness. Earlier reports have studied the effect of the physical microenvironment such as stiffness in the regulation of cell area. In particular, Collins et al. functionalized E-cadherin-Fc on PAA gels to assess the role of E-cadherin adhesion of MDCK cells in rigidity sensing [46]. It was found that the substrate stiffness regulated the cell spreading area. This result is in agreement with the results of C2 myogenic cells on N-cadherin coated micropillar assay [43]. In addition, substrate stiffness influences the cell morphology; it was reported that the cells on stiffer substrates are more circular compared to cells on softer substrates [46].

Actin dynamics and structure is one of the factors that contributes to cell morphology. It was found that cell protrusion velocity decreased with increasing the substrate rigidity [46]. Such altered protrusive activity on the rigid substrate is due to the effect of altered

actin structure and adhesion organization. In particular, it was found that the epithelial cells on more rigid E-cadherin coated substrates possess robust radial actin structures at proximal end as well as prominent large E-cadherin mediated adhesion. These results suggest that the formation of E-cadherin adhesion as well as actin organization are aspects of cell response to substrate rigidity.

Cell division is one of the aspects that controls organ size and is regulated by mechanical cues. The transcription factor YAP (yes-associated protein) is a mechanosensor which is found in many cell types such as epithelial cells. YAP nuclear recruitment is a key signaling event that promotes proliferation. The nuclear accumulation of YAP is regulated by cell ECM rigidity and cell spreading area [94, 95]. In particular, cells on stiffer substrates are larger and promote YAP nuclear accumulation. In contrast, cells on soft substrates are smaller and induce YAP cytoplasmic retention. In addition to YAP responses to the microenvironment, YAP is also regulated by actin filament structure [41]. In particular, cells with prominent actin expression level have more YAP nuclear accumulation. Moreover, cell density also influences YAP localization. It was found that higher cell population density promotes YAP cytoplasmic retention whereas YAP is localized in the nucleus in sparse cells [93].

## 4.2 Methods

### Pharmacological Inhibition

The formin inhibitor SMIFH2 and Arp2/3 inhibitor CK-666 were purchased from Sigma-Aldrich, Burlington, MA. C2bbe cells already plated for 2 hours in serum free medium were treated with 100 μM CK-666 and 20 μM SMIFH2 for 2 hours prior to fixation. For

stabilizing actin filaments, 1 nM of jasplakinolide was used for 1 hour. Anti-phosphorylated myosin light chain Serine19 (Cell Signaling Technology) was used for staining phosphomyosin.

## 4.3 Results

### 4.3.1 Effect of E-cadherin-coated cell-like substrates on E-cadherin adhesion organization

We wanted to employ an experimental model to restrict the C2bbe cells to E-cadherin adhesion without formation of focal adhesions. Therefore, we prepared oriented immobilized E-cadherin-Fc on soft silicones of stiffness 0.4, 2.4 and 8.7 kPa, which was explained in Chapter 3. The substrates coated with E-cadherin-Fc mimic the cell-cell interactions due to E-cadherin binding. We seeded C2bbe cells on the E-cadherin-Fc coated substrates in serum-free conditions and then performed immunofluorescence in 2 hrs. We first quantified the cell spreading area for each substrate stiffnesses (Figure 23). It is evident that cell area is not sensitive to substrate stiffness ($p = 0.65$) in contrast to previous reports for E-cadherin [46] and N-cadherin surfaces [43].

Next, we examined the E-cadherin adhesions by immunofluorescence staining of β-catenin of the cells on the different substrates. By comparing the β-catenin staining, we identified two main types of E-cadherin adhesions - nascent adhesions and linear adhesions. Nascent adhesions are dot-like small adhesions (~0.2 μm wide) whereas linear adhesions were radially oriented, larger, and close to the cell edge (Figure 24).

We then sought to determine the fraction of cells that exhibited linear and just nascent adhesions on the three substrate stiffnesses. As shown in Figure 25, the number of cells

exhibiting linear adhesion increases with substrate rigidity, which is in an agreement with previous reports [43, 46]. Interestingly, by increasing the substrate stiffness, smaller fraction of cells exhibit nascent adhesions. This result suggests that C2bbe cells display prominent linear adhesions in a stiffer microenvironment.

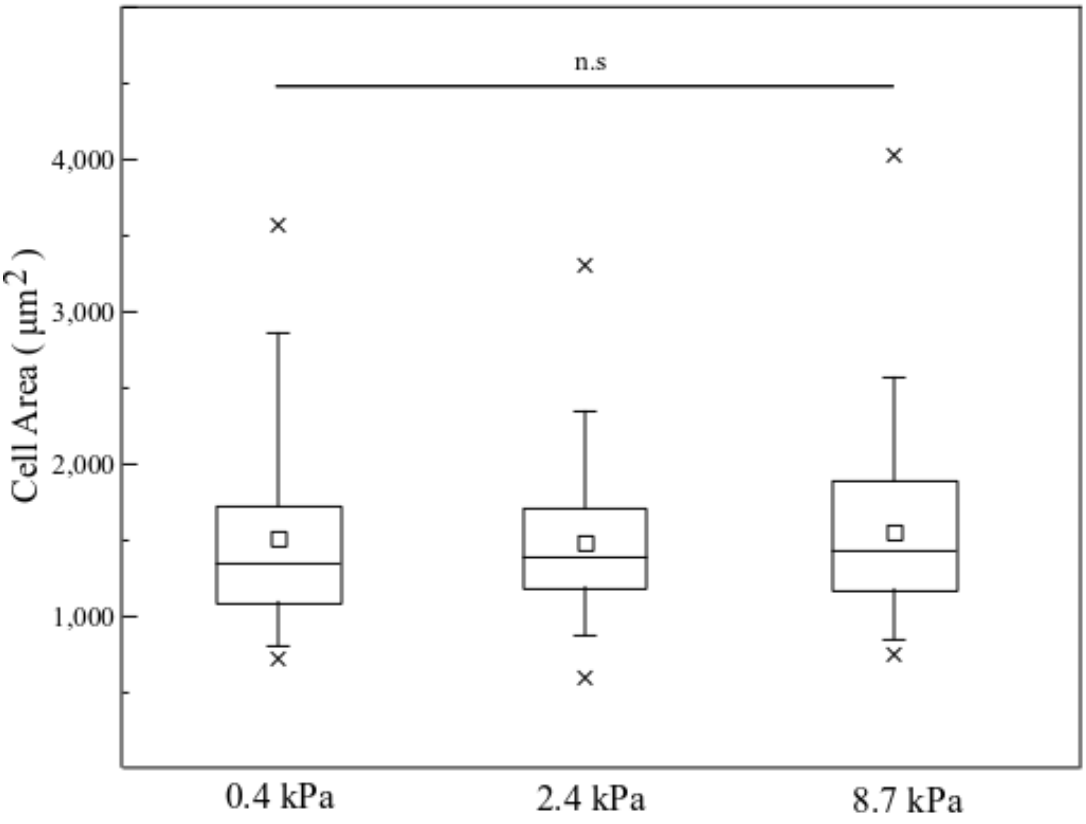


Figure 23. Cell area is independent of substrate stiffness for cell-like E-cadherin substrates. Box plots comparing the cell spreading area on 3 substrates. In the box plots, the small square represents the mean, the horizontal line represents the median, cross (x) represents minimum and maximum value, lower and upper sides of the large box represent the 25 and 75 percentile values and whiskers represent 5 and 95 percentile values.

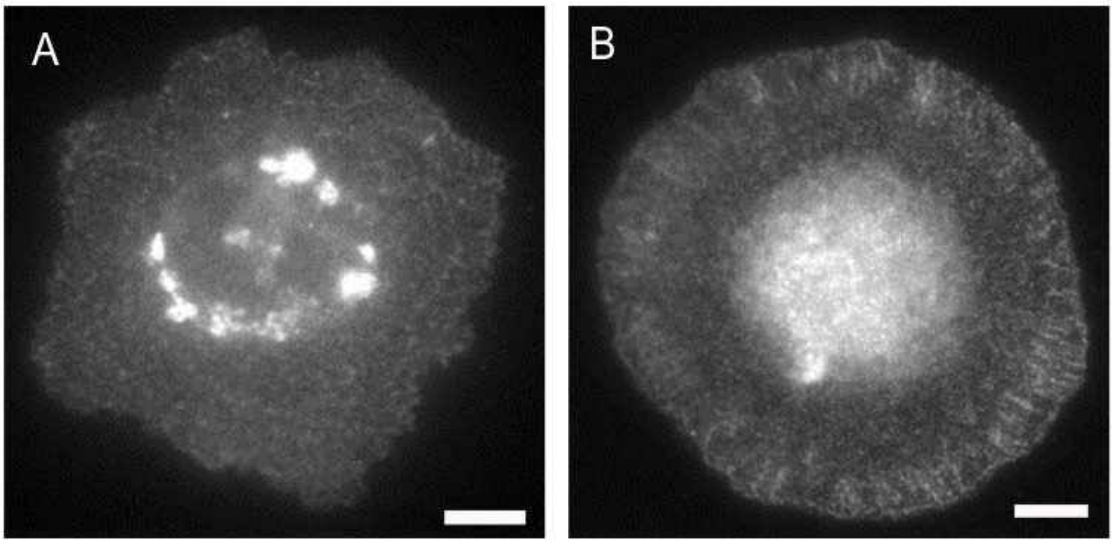


Figure 24. Formation of different adhesion types on oriented immobilized E-cadherin substrates. Representative immunofluorescence images of C2bbe cells plated on oriented E-cadherin 8.7 kPa silicone, stained for β-catenin, which exhibit just nascent adhesions (A) or linear adhesions (B) (Scale bar: 5 μm).

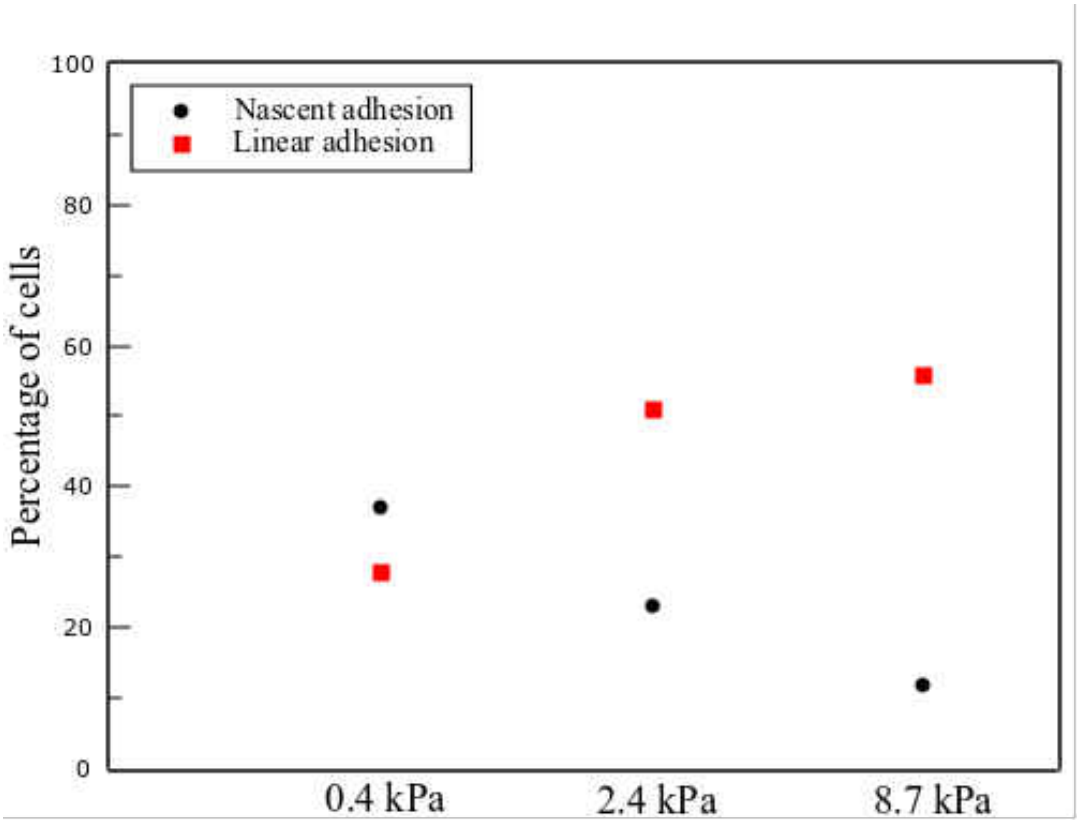


Figure 25. Fraction of cells exhibiting linear adhesions or just nascent E-cadherin adhesions is substrate stiffness dependent. Linear and nascent adhesions displaying cell fractions are shown in red squares and black circles respectively.

### 4.3.2 Effect of E-cadherin-coated cell-like substrates on YAP localization

Previous studies have reported that the YAP transcriptional activity is regulated by mechanical cues [94]. To assess if YAP recruitment in C2bbe cells is regulated by substrate rigidity, immunofluorescence images of YAP and the corresponding cell nucleus were acquired for each 0.4 kPa (Figure 26A-B), 2.4 kPa (Figure 26C-D) and 8.7 kPa (Figure 26E-F) substrate. We visually observed that YAP is mainly localized in the nucleus regardless of substrate stiffness. Then, we analyzed the immunofluorescence images of YAP images by quantifying the average intensity of YAP in the nucleus and

divided it by the average intensity of YAP in cytoplasm to assess the degree of nuclear recruitment. By comparing the YAP nuclear/cytoplasmic intensity ratio, we found that YAP nuclear accumulation was statistically independent of substrate rigidity ($p = 0.1$) which is somewhat in contrast to what was previously reported [94]. In general, adherent cells adapt larger spreading areas on stiffer substrate and thus modulate YAP nuclear localization. However, in our case, cell spreading area did not change with the considered range of substrate rigidity (Figure 23), indicating that YAP nuclear activity is regulated primarily by cell spreading area.

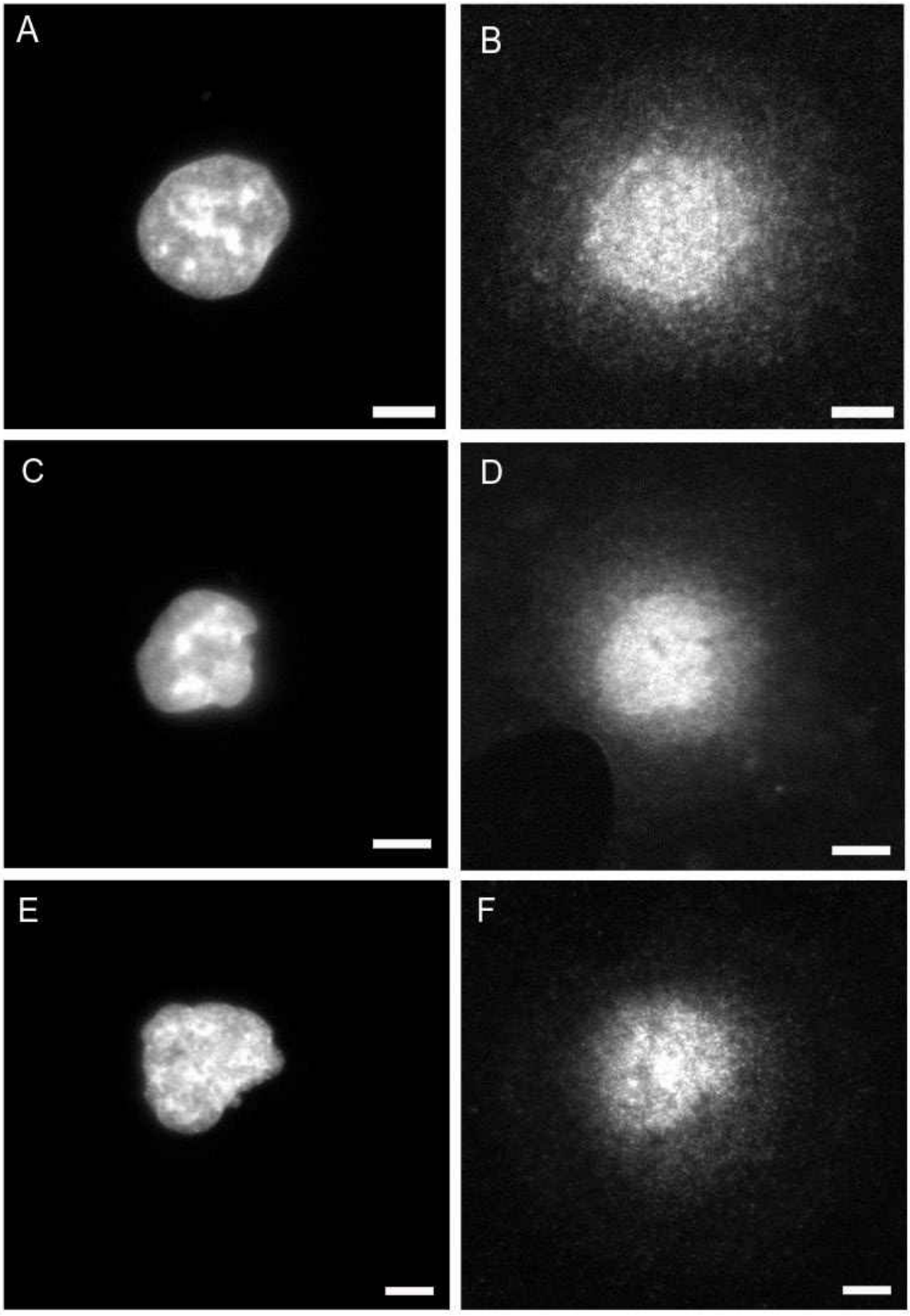

Figure 26. YAP is mainly accumulated in nucleus independent of substrate rigidity. Representative immunofluorescence images of DAPI (left panels) and corresponding YAP (right panels) for 0.4 kPa (A,B), 2.4 kPa (C,D) and 8.7 kPa (E,F) E-cadherin substrates. (Scale bar: 5 μm).

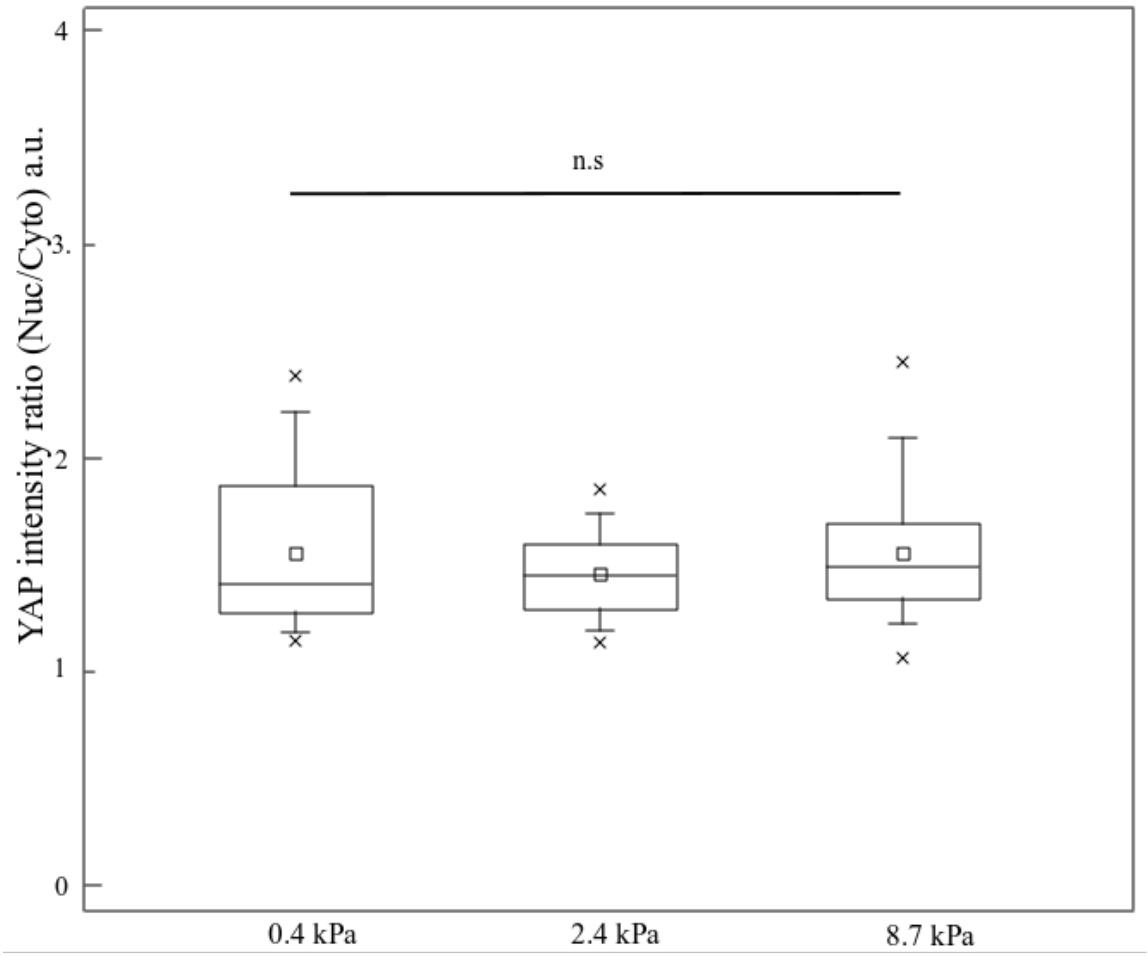


Figure 27. YAP transcriptional activity is independent of substrate stiffness. Box plots comparing the YAP average intensity ratio on 3 substrates. In the box plots, the small square represents the mean, the horizontal line represents the median, cross (x) represents minimum and maximum value, lower and upper sides of the large box represent the 25 and 75 percentile values and whiskers represent 5 and 95 percentile values.

### 4.3.3 Effect of actin organization on E-cadherin adhesions on E-cadherin-coated cell-like substrates

We wanted to determine as to what factors influence the formation of E-cadherin adhesions on cell-like soft substrates. We had observed that a larger fraction of cells on the stiffer substrate exhibited linear adhesion. Immunofluorescence staining of actin filaments shows that cells on soft substrates (0.4 kPa) display circumferential actin structures (Figure 28A) whereas radial actin structures are also associated with circumferential actin bundles (Figure 28C) for the cells on stiff substrate (8.7 kPa). Moreover, radially oriented actin bundles were directed towards and linked to linear E-cadherin adhesions (Figure 28D). These results suggest that actin organization was correlated to E-cadherin adhesion organization.

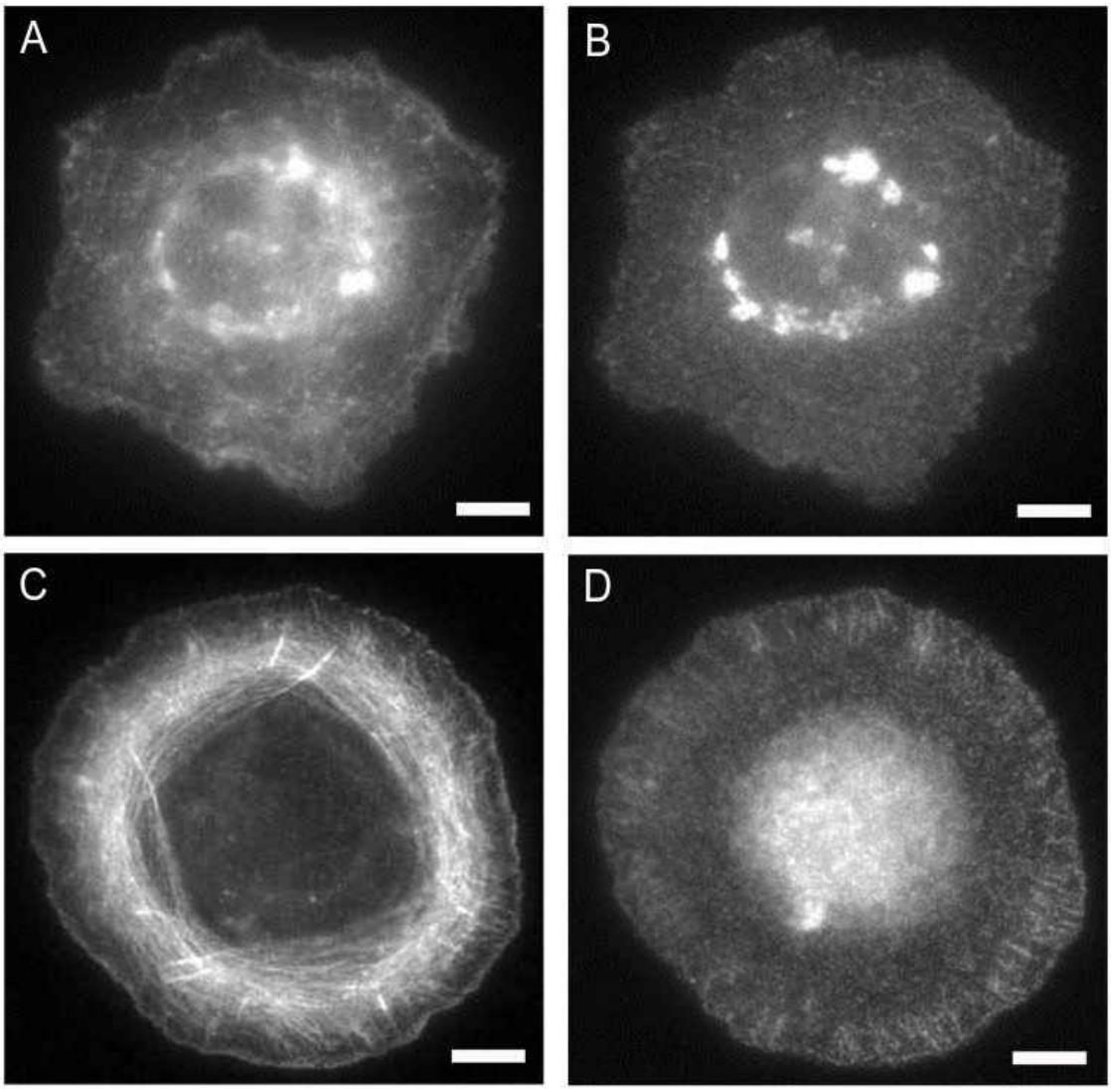


Figure 28. E-cadherin adhesion organization is correlated with actin structure. Immunofluorescence images of actin (left panels) and β-catenin (right panels) of C2bbe cells plated on oriented E-cadherin-Fc coated 8.7 kPa substrate (Scale bar: 5 μm).

### 4.3.4 Phosphomyosin localization in cells on E-cadherin-coated cell-like substrates

We then sought to determine if circumferential actin structures are contractile. The actomyosin apparatus is response for cell contractility. Myosin motors bind to actin filaments and generate contractile tension if phosphorylated [96]. In this context, we

assessed myosin activity by immunofluorescence staining of the phospho-myosin light chain. As shown in Figure 29, phospho-myosin (indicating active myosin) is localized at actin structures and that implies that circumferential actin bundles are contractile.

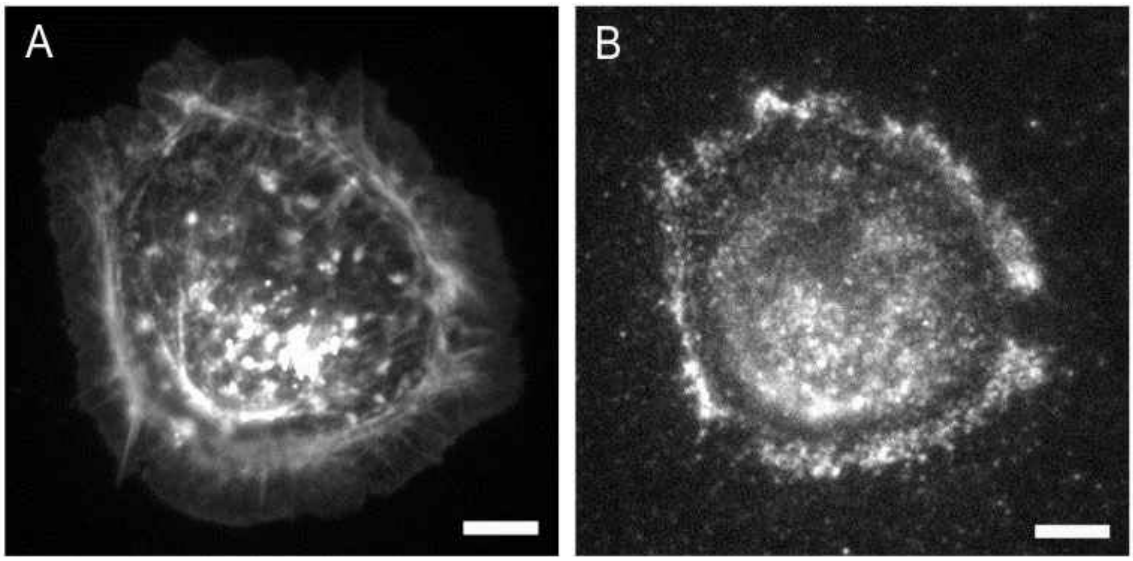


Figure 29. Circumferential actin structures display phosphomyosin localization. Representative immunofluorescence images of C2bbe cells plated on 8.7 kPa substrate stained for actin (A) and p-myosin (B). (Scale bar: 5 μm).

### 4.3.5 Effect of formin inhibition on actin organization and E-cadherin adhesions on E-cadherin-coated cell-like substrates

We wanted to determine whether differences in actin structure organization and E-cadherin adhesion organization were mediated by actin nucleating proteins. C2bbe cells on oriented, immobilized E-cadherin-Fc coated 8.7 kPa substrate displayed prominent linear radially oriented actin structures integrated with circumferential actin structures. Therefore, we tested if the actin nucleator formin influences the actin structure and E-cadherin adhesion organization. Accordingly, C2bbe cells under formin inhibition (20

μM of SMIFH2) did not display radial actin, but only circumferential actin structures. In addition, the extent of circumferential actin was diminished in formin inhibited cells, as shown in Figure 30 A,C. We further investigated if formin inhibited cells showed changes in E-cadherin adhesion characteristics. Immunofluorescence images of β-catenin show that the formin inhibited cells display more nascent adhesions, presumably due to absence of radial actin structures and decrease in circumferential actin structures (Figure 30B).

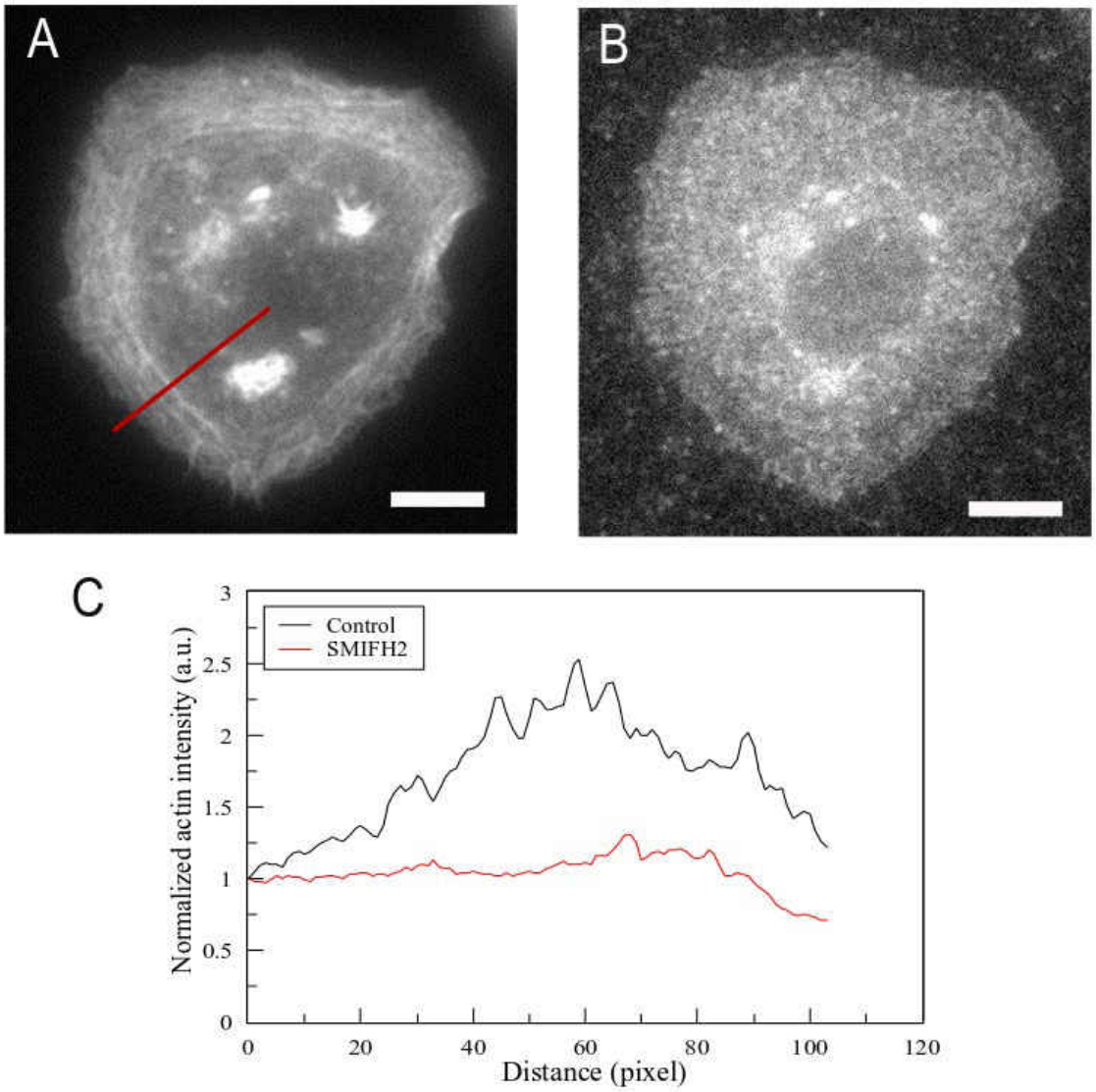

Figure 30. Linear E-cadherin adhesions are formin dependent. Immunofluorescence images of SMIFH2-treated C2bbe cells, plated on oriented E-cadherin-Fc coated on 8.7 kPa substrate stained for actin (A) and β-catenin (B). Normalized fluorescence intensity of actin for control and SMIFH2-treated cells. The red line in panel A corresponds to measured actin intensity of SMIFH2-treated cells. (Scale bar: 5 μm).

### 4.3.6 Effect of Arp2/3 inhibition on actin organization and E-cadherin adhesions on E-cadherin-coated cell-like substrates

The Arp2/3 complex is another major actin nucleator, responsible for nucleating actin branches [97]. We thus used a pharmacological inhibitor of Arp2/3 (CK-666) to test the role of this actin nucleator in the observed actin structures. We found that neither actin nor E-cadherin organization was altered under Arp2/3 inhibition (Figure 31A-B).

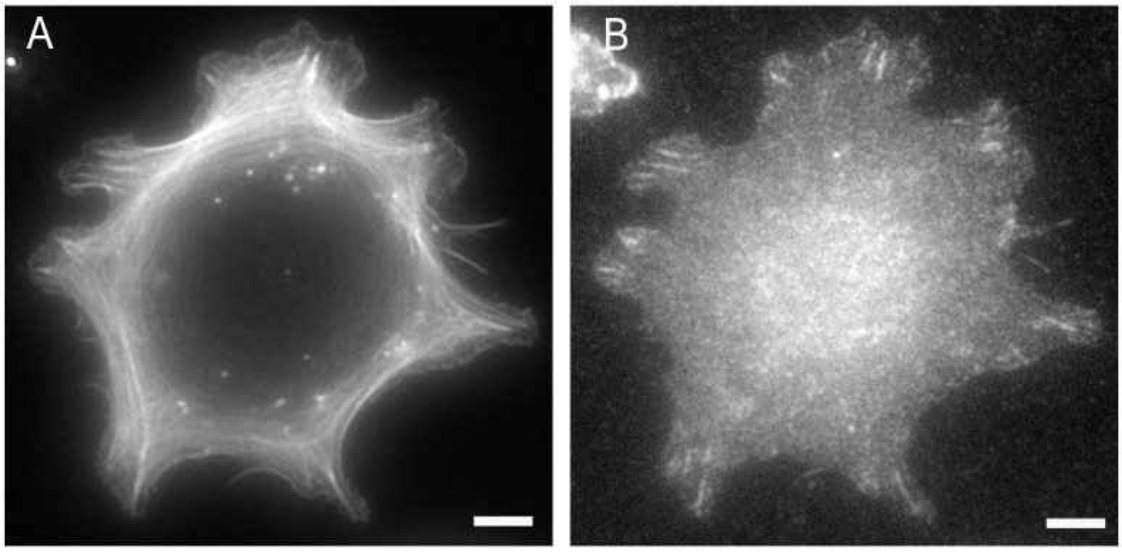


Figure 31. E-cadherin adhesion on cell-like soft E-cadherin substrates is largely Arp2/3 independent. Immunofluorescence images of CK-666-treated C2bbe cells, plated on

oriented E-cadherin-Fc coated on 8.7 kPa substrate stained for actin (A) and β-catenin (B) (Scale bar: 5 μm).

Our results suggest that when radial actin structures are integrated with circumferential contractile actin structures, the C2bbe cells display linear adhesions. In addition to linear and nascent adhesions, we found a small fraction of C2bbe cells exhibiting clump-like large adhesions on oriented E-cadherin-Fc coated substrates. Such clump adhesions were localized with clumps (localized regions of high intensity) of actin (Figure 32). The actin clumps are presumably due to phosphomyosin mediated contractility.

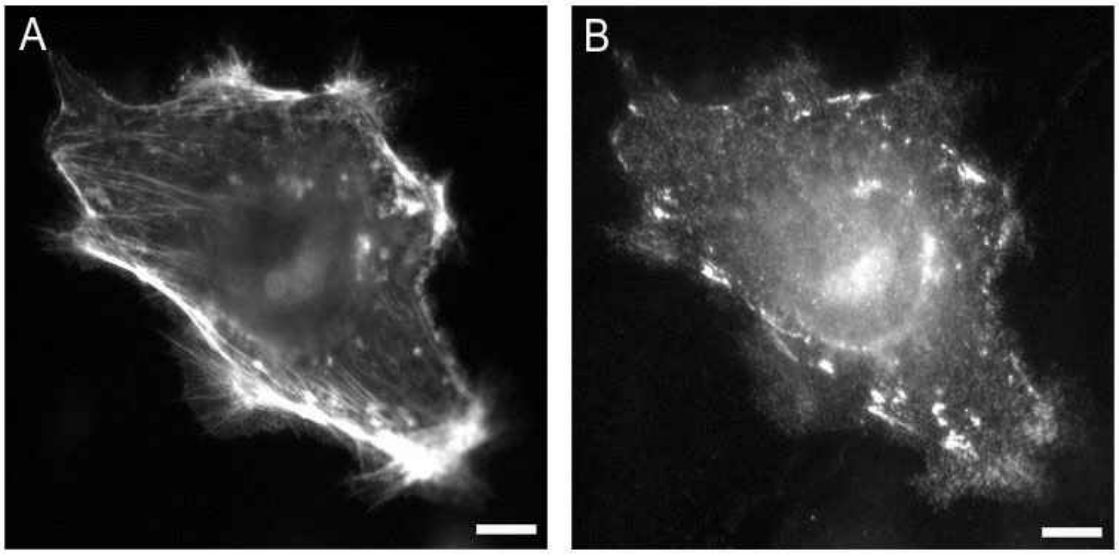


Figure 32. Adhesion clumps are localized at actin clumps. Immunofluorescence images of C2bbe cells plated on oriented E-cadherin-Fc coated on 8.7 kPa substrate stained for actin (A) and β-catenin (B) (Scale bar: 5 μm).

### 4.3.7 Effect of actin stabilization on E-cadherin adhesions on E-cadherin-coated cell-like substrates

We thus wanted to investigate whether the adhesion clump formation is just due to force generation by actomyosin or if just localized higher actin density can also promote it. Jasplakinolide is a chemical isolated from a marine sponge that stabilizes and promotes actin polymerization [98]. In order to assess if the adhesion clumps can be caused by just actin accumulation, we used jasplakinolide to stabilize the actin clusters [99]. The immunofluorescence image of actin in Figure 33A shows that jasplakinolide can dramatically affect actin structure. Moreover, E-cadherin adhesion clumps are co-localized with these actin clumps. (Figure 33B). Thus, jasplakinolide treatment provides convincing evidence that local higher density of actin structures promotes E-cadherin adhesion clumps.

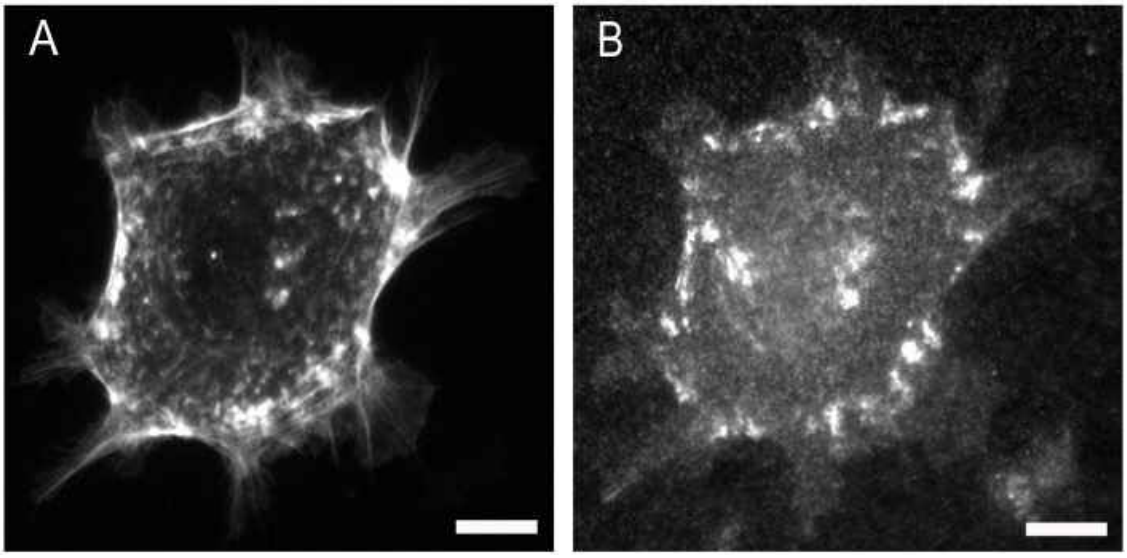


Figure 33. E-cadherin adhesion clumps induced by stabilizing actin filaments. Immunofluorescence images of jasplakinolide treated C2bbe cells, plated on oriented E-

cadherin-Fc coated on 8.7 kPa substrate stained for actin (A) and β-catenin (B) (Scale bar: 5 μm).

### 4.3.8 Overall model of actin-dependent E-cadherin organization on E-cadherin-coated cell-like substrates

Together, our results indicated that linear E-cadherin adhesion formation is substrate stiffness dependent. Such linear adhesion formation was mediated by radially oriented actin structures integrated with contractile circumferential actin structures. Furthermore, cells under formin inhibition, do not exhibit linear adhesions. On the other hand, nascent adhesions did not require specifically oriented actin structures, as expected. Therefore, the correlation between actin structure and E-cadherin adhesion in cell-like stiffness microenvironments can be explained in Figure 34.

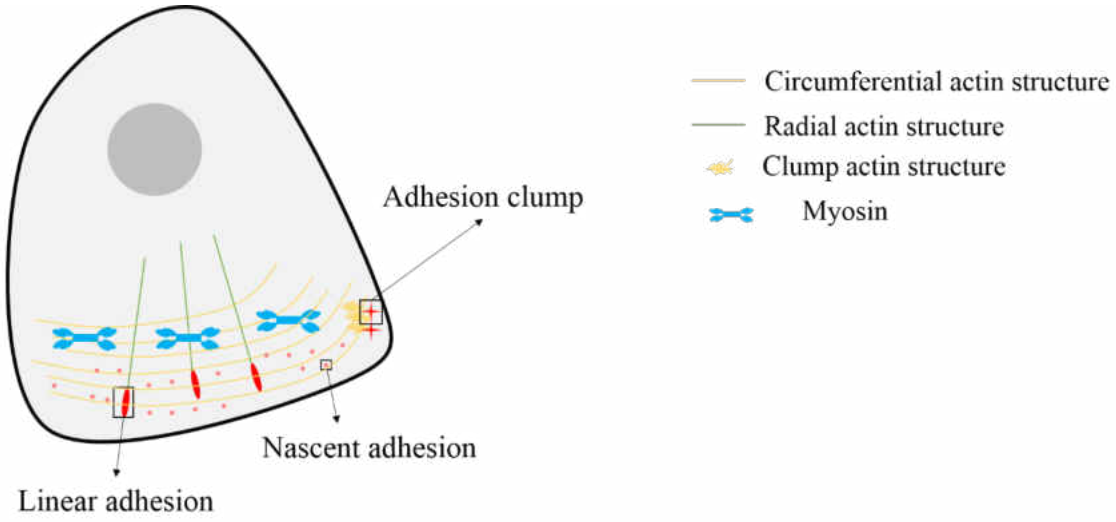


Figure 34. Schematic model of E-cadherin adhesion types on oriented E-cadherin-Fc coated substrate with cell-like stiffness. Linear adhesions are mediated by radial actin filaments integrated with contractile circumferential actin filaments but nascent adhesions

do not require oriented actin structures. Adhesion clumps form with local actin accumulation due to contractility.

# CHAPTER 5

# CONCLUSION AND SCOPE FOR FUTURE WORK

Adherent cells interact with their microenvironment at cell-ECM and cell-cell interfaces using their adhesions and exerted contractile forces. Therefore, it is important to study the effect of microenvironmental physical factors such as geometry and stiffness in regulating the cell adhesion and contractility. In this dissertation, we have considered two representative situations: the effect of microenvironmental geometry and stiffness on fibroblast force generation and the effect of microenvironmental stiffness on E-cadherin adhesion.

Fibroblasts in connective tissue interact with their fibrillar microenvironment and often mechanically respond to their microenvironment by exerting contractile forces. As detailed in Chapter 2, we have developed an experimental model to maintain fibroblasts in fibrillar morphology. We have quantified the fibrillar force exerted by fibroblasts for different microenvironmental stiffness. In contrast with fibroblasts with 2D morphology, the fibrillar fibroblasts exerted forces that were independent of substrate stiffness. The difference in outcomes between 2D (reported previously) and 1D may be due to the different actin architectures in the two cases. Accordingly, we found that not only the fibrillar length, but also fibrillar forces depend on formin family of nucleators. In the future, it will be important to determine what factors other than formins modulate force generation in fibrillar fibroblasts. Furthermore, it will be important to determine if inter-connected 1D lines may show some dependence on substrate stiffness, as the cells can spread in between the lines close to the junction between 2 lines. Such experimental

models can increase in complexity in order to more closely mimic the situation in 3D ECM *in vivo*.

In epithelial tissues, epithelial cells not only adhere to ECM, but also form cell-cell contacts via E-cadherin receptors to maintain tissue integrity. In order to investigate the role E-cadherin itself plays in sensing the microenvironment, we have fabricated and characterized soft substrates with cell-like stiffness coated with oriented immobilized E-cadherin-Fc to mimic the cell-cell interaction of epithelial cells *in vivo*. We found that cell spread area as well as YAP nuclear localization are independent of substrate stiffness in apparent contrast to what was found in previous reports. The difference could be due to the fact that we are considering E-cadherin-based surfaces within a narrow range of relevance. Here, cell spread area was independent substrate stiffness. This also suggests that cell spread area primarily regulates YAP activity. On the other hand, we found that E-cadherin adhesion formation is highly dependent on substrate stiffness due to the fact that larger fraction of cells exhibited linear E-cadherin adhesions at higher stiffness, whereas cells on softer substrates just exhibit nascent E-cadherin adhesions. We further found that linear adhesions are supported by radial actin structures which are integrated with contractile circumferential actin structures. We also found that formin plays a key role in regulating E-cadherin adhesions. Our observations enabled us to propose a model for E-cadherin adhesion regulation in the context of cell-like microenvironmental stiffness. This experimental model can enable the study of E-cadherin adhesions in a more native context in the future, including assessment of the role of various constituents of the proposed E-cadherin mechanotransduction apparatus in adhesion and force generation.

Taken together, our studies highlight the unique role played by physical characteristics of the micro-environment in different contexts: The fact that rigidity of the microenvironment did not affect the fibrillar forces suggests that cell geometry primarily influences cell force exertion in fibrillar fibroblasts. On the other hand, our results on E-cadherin mechanosensitivity suggest that, even though the cell-like stiffness of the microenvironment did not influence the cell spreading area, it does play an essential role in the modulation of E-cadherin adhesions.

## REFERENCES


1. DiMilla, P.A., et al., *Maximal migration of human smooth muscle cells on fibronectin and type IV collagen occurs at an intermediate attachment strength.* J Cell Biol, 1993. **122**(3): p. 729-37.
2. Ridley, A.J., et al., *Cell Migration: Integrating Signals from Front to Back.* Science, 2003. **302**(5651): p. 1704-1709.
3. Zaman, M.H., et al., *Migration of tumor cells in 3D matrices is governed by matrix stiffness along with cell-matrix adhesion and proteolysis.* Proceedings of the National Academy of Sciences, 2006. **103**(29): p. 10889-10894.
4. Doyle, A.D., et al., *One-dimensional topography underlies three-dimensional fibrillar cell migration.* The Journal of Cell Biology, 2009. **184**(4): p. 481-490.
5. Lukashev, M.E. and Z. Werb, *ECM signalling: orchestrating cell behaviour and misbehaviour.* Trends in Cell Biology, 1998. **8**(11): p. 437-441.
6. Ghousifam, N., et al., *A three-dimensional in vitro model to demonstrate the haptotactic effect of monocyte chemoattractant protein-1 on atherosclerosis-associated monocyte migration.* International Journal of Biological Macromolecules, 2017. **97**: p. 141-147.
7. Ozkan, A., et al., *In vitro vascularized liver and tumor tissue microenvironments on a chip for dynamic determination of nanoparticle transport and toxicity.* Biotechnology and Bioengineering, 2019. **116**(5): p. 1201-1219.
8. Rozario, T. and D.W. DeSimone, *The extracellular matrix in development and morphogenesis: a dynamic view.* Dev Biol, 2010. **341**(1): p. 126-40.
9. Wise, S.G. and A.S. Weiss, *Tropoelastin.* The International Journal of Biochemistry & Cell Biology, 2009. **41**(3): p. 494-497.
10. Frantz, C., K.M. Stewart, and V.M. Weaver, *The extracellular matrix at a glance.* J Cell Sci, 2010. **123**(24): p. 4195-4200.
11. Hynes, R.O., *Integrins: bidirectional, allosteric signaling machines.* cell, 2002. **110**(6): p. 673-687.
12. Califano, J.P. and C.A. Reinhart-King, *Substrate Stiffness and Cell Area Predict Cellular Traction Stresses in Single Cells and Cells in Contact.* Cellular and Molecular Bioengineering, 2010. **3**(1): p. 68-75.
13. Discher, D.E., P. Janmey, and Y.-l. Wang, *Tissue Cells Feel and Respond to the Stiffness of Their Substrate.* Science, 2005. **310**(5751): p. 1139-1143.
14. Wolf, K., et al., *Physical limits of cell migration: Control by ECM space and nuclear deformation and tuning by proteolysis and traction force.* The Journal of Cell Biology, 2013. **201**(7): p. 1069-1084.
15. Roeder, B.A., K. Kokini, and S.L. Voytik-Harbin, *Fibril Microstructure Affects Strain Transmission Within Collagen Extracellular Matrices.* Journal of Biomechanical Engineering, 2009. **131**(3).

16. Guthold, M., et al., *A Comparison of the Mechanical and Structural Properties of Fibrin Fibers with Other Protein Fibers.* Cell Biochemistry and Biophysics, 2007. **49**(3): p. 165-181.

17. An, K.N., Y.L. Sun, and Z.P. Luo, *Flexibility of type I collagen and mechanical property of connective tissue.* Biorheology, 2004. **41**(3-4): p. 239-46.

18. Pedersen, J.A. and M.A. Swartz, *Mechanobiology in the Third Dimension.* Annals of Biomedical Engineering, 2005. **33**(11): p. 1469-1490.

19. Seetharaman, S. and S. Etienne-Manneville, *Integrin diversity brings specificity in mechanotransduction.* Biology of the Cell, 2018. **110**(3): p. 49-64.

20. Handorf, A.M., et al., *Tissue stiffness dictates development, homeostasis, and disease progression.* Organogenesis, 2015. **11**(1): p. 1-15.

21. Moeendarbary, E. and A.R. Harris, *Cell mechanics: principles, practices, and prospects.* Wiley Interdisciplinary Reviews: Systems Biology and Medicine, 2014. **6**(5): p. 371-388.

22. Solon, J., et al., *Fibroblast adaptation and stiffness matching to soft elastic substrates.* Biophysical journal, 2007. **93**(12): p. 4453-4461.

23. Ketene, A.N., et al., *The effects of cancer progression on the viscoelasticity of ovarian cell cytoskeleton structures.* Nanomedicine, 2012. **8**(1): p. 93-102.

24. Berdyyeva, T.K., C.D. Woodworth, and I. Sokolov, *Human epithelial cells increase their rigidity with ageing in vitro: direct measurements.* Phys Med Biol, 2005. **50**(1): p. 81-92.

25. Matzke, R., K. Jacobson, and M. Radmacher, *Direct, high-resolution measurement of furrow stiffening during division of adherent cells.* Nat Cell Biol, 2001. **3**(6): p. 607-10.

26. Agus, D.B., et al., *A physical sciences network characterization of non-tumorigenic and metastatic cells.* Sci Rep, 2013. **3**: p. 1449.

27. Rebelo, L.M., et al., *Comparison of the viscoelastic properties of cells from different kidney cancer phenotypes measured with atomic force microscopy.* Nanotechnology, 2013. **24**(5): p. 055102.

28. Faria, E.C., et al., *Measurement of elastic properties of prostate cancer cells using AFM.* Analyst, 2008. **133**(11): p. 1498-500.

29. Spence, E.F. and S.H. Soderling, *Actin out: regulation of the synaptic cytoskeleton.* Journal of Biological Chemistry, 2015. **290**(48): p. 28613-28622.

30. Martino, F., et al., *Cellular Mechanotransduction: From Tension to Function.* Frontiers in Physiology, 2018. **9**(824).

31. Lessey, E.C., C. Guilluy, and K. Burridge, *From mechanical force to RhoA activation.* Biochemistry, 2012. **51**(38): p. 7420-7432.

32. Plotnikov, S.V., et al., *Force fluctuations within focal adhesions mediate ECM-rigidity sensing to guide directed cell migration.* Cell, 2012. **151**(7): p. 1513-27.

33. Oakes, Patrick W., et al., *Geometry Regulates Traction Stresses in Adherent Cells.* Biophysical Journal, 2014. **107**(4): p. 825-833.

34. Oakes, P.W., et al., *Tension is required but not sufficient for focal adhesion maturation without a stress fiber template.* The Journal of Cell Biology, 2012. **196**(3): p. 363-374.

35. Dumbauld, D.W., et al., *How vinculin regulates force transmission.* Proceedings of the National Academy of Sciences, 2013. **110**(24): p. 9788-9793.

36. Han, Sangyoon J., et al., *Decoupling Substrate Stiffness, Spread Area, and Micropost Density: A Close Spatial Relationship between Traction Forces and Focal Adhesions.* Biophysical Journal, 2012. **103**(4): p. 640-648.

37. Eftekharjoo, M., et al., *Fibrillar force generation by fibroblasts depends on formin.* Biochemical and biophysical research communications, 2019. **510**(1): p. 72-77.

38. Wang, X. and T. Ha, *Defining single molecular forces required to activate integrin and notch signaling.* Science, 2013. **340**(6135): p. 991-994.

39. Chowdhury, F., et al., *Single molecular force across single integrins dictates cell spreading.* Integrative Biology, 2015. **7**(10): p. 1265-1271.

40. Gumbiner, B.M., *Regulation of cadherin adhesive activity.* The Journal of cell biology, 2000. **148**(3): p. 399-404.

41. Heisenberg, C.-P. and Y. Bellaïche, *Forces in tissue morphogenesis and patterning.* Cell, 2013. **153**(5): p. 948-962.

42. Krishnan, R., et al., *Substrate stiffening promotes endothelial monolayer disruption through enhanced physical forces.* American Journal of Physiology-Cell Physiology, 2010. **300**(1): p. C146-C154.

43. Ladoux, B., et al., *Strength Dependence of Cadherin-Mediated Adhesions.* Biophysical Journal, 2010. **98**(4): p. 534-542.

44. Leckband, D.E., et al., *Mechanotransduction at cadherin-mediated adhesions.* Current opinion in cell biology, 2011. **23**(5): p. 523-530.

45. Ladoux, B., et al., *The mechanotransduction machinery at work at adherens junctions.* Integrative Biology, 2015. **7**(10): p. 1109-1119.

46. Collins, C., et al., *Changes in E-cadherin rigidity sensing regulate cell adhesion.* Proceedings of the National Academy of Sciences, 2017. **114**(29): p. E5835-E5844.

47. Polio, S.R., et al., *A micropatterning and image processing approach to simplify measurement of cellular traction forces.* Acta biomaterialia, 2012. **8**(1): p. 82-88.

48. Maruthamuthu, V., et al., *Cell-ECM traction force modulates endogenous tension at cell–cell contacts.* Proceedings of the National Academy of Sciences, 2011. **108**(12): p. 4708-4713.

49. Butler, J.P., et al., *Traction fields, moments, and strain energy that cells exert on their surroundings.* American Journal of Physiology-Cell Physiology, 2002. **282**(3): p. C595-C605.

50. Macke, W., *L. D. Landau and E. M. Lifshitz Mechanics. Vol. 1 of: Course of Theoretical Physics. 165 S. m. 55 Abb. Oxford/London/Paris 1960. Pergamon Press Ltd. Preis geb. 40 s. net.* ZAMM - Journal of Applied Mathematics and Mechanics / Zeitschrift für Angewandte Mathematik und Mechanik, 1961. **41**(9): p. 392-392.

51. Vogel, V. and M. Sheetz, *Local force and geometry sensing regulate cell functions.* Nat Rev Mol Cell Biol, 2006. **7**(4): p. 265-75.

52. Oakes, P.W., et al., *Geometry regulates traction stresses in adherent cells.* Biophys J, 2014. **107**(4): p. 825-33.

53. Han, S.J., et al., *Decoupling substrate stiffness, spread area, and micropost density: a close spatial relationship between traction forces and focal adhesions.* Biophys J, 2012. **103**(4): p. 640-8.

54. Doyle, A.D. and K.M. Yamada, *Mechanosensing via cell-matrix adhesions in 3D microenvironments.* Exp Cell Res, 2016. **343**(1): p. 60-66.

55. Gjorevski, N., et al., *Dynamic tensile forces drive collective cell migration through three-dimensional extracellular matrices.* Sci Rep, 2015. **5**: p. 11458.

56. Doyle, A.D., et al., *Dimensions in cell migration.* Curr Opin Cell Biol, 2013. **25**(5): p. 642-9.

57. Sheets, K., et al., *Nanonet Force Microscopy for Measuring Cell Forces.* Biophys J, 2016. **111**(1): p. 197-207.

58. Doyle, A.D., et al., *Micro-environmental control of cell migration--myosin IIA is required for efficient migration in fibrillar environments through control of cell adhesion dynamics.* J Cell Sci, 2012. **125**(Pt 9): p. 2244-56.

59. Hall, A., et al., *Nanonet force microscopy for measuring forces in single smooth muscle cells of the human aorta.* Mol Biol Cell, 2017. **28**(14): p. 1894-1900.

60. Han, S.J., et al., *Spatial and temporal coordination of traction forces in one-dimensional cell migration.* Cell Adh Migr, 2016. **10**(5): p. 529-539.

61. Wells, R.G., *Tissue mechanics and fibrosis.* Biochim Biophys Acta, 2013. **1832**(7): p. 884-90.

62. Guetta-Terrier, C., et al., *Protrusive waves guide 3D cell migration along nanofibers.* J Cell Biol, 2015. **211**(3): p. 683-701.

63. Zigmond, S.H., *Formin-induced nucleation of actin filaments.* Curr Opin Cell Biol, 2004. **16**(1): p. 99-105.

64. Yeung, T., et al., *Effects of substrate stiffness on cell morphology, cytoskeletal structure, and adhesion.* Cytoskeleton, 2005. **60**(1): p. 24-34.

65. Maruthamuthu, V., et al., *Cell-ECM traction force modulates endogenous tension at cell-cell contacts.* Proc Natl Acad Sci U S A, 2011. **108**(12): p. 4708-13.

66. Maruthamuthu, V. and M.L. Gardel, *Protrusive activity guides changes in cell-cell tension during epithelial cell scattering.* Biophys J, 2014. **107**(3): p. 555-63.

67. Martiel, J.L., et al., *Measurement of cell traction forces with ImageJ.* Methods Cell Biol, 2015. **125**: p. 269-87.

68. Butler, J.P., et al., *Traction fields, moments, and strain energy that cells exert on their surroundings.* American Journal of Physiology-Cell Physiology, 2002. **282**(3): p. C595-C605.

69. Plotnikov, S.V., et al., *High-resolution traction force microscopy.* Methods Cell Biol, 2014. **123**: p. 367-94.

70. Sabass, B., et al., *High resolution traction force microscopy based on experimental and computational advances.* Biophys J, 2008. **94**(1): p. 207-20.

71. Schwarz, U.S., et al., *Calculation of Forces at Focal Adhesions from Elastic Substrate Data: The Effect of Localized Force and the Need for Regularization.* Biophysical Journal, 2002. **83**(3): p. 1380-1394.

72. Muhamed, I., F. Chowdhury, and V. Maruthamuthu, *Biophysical Tools to Study Cellular Mechanotransduction.* Bioengineering, 2017. **4**(1): p. 12.

73. Leal-Egana, A., et al., *The size-speed-force relationship governs migratory cell response to tumorigenic factors.* Mol Biol Cell, 2017. **28**(12): p. 1612-1621.

74. Ray, A., et al., *Anisotropic forces from spatially constrained focal adhesions mediate contact guidance directed cell migration.* Nat Commun, 2017. **8**: p. 14923.

75. Lo, C.M., Wang, H. B., Dembo, M., and Wang, Y. L., *Cell movement is guided by the rigidity of the substrate.* Biophysical Journal, 2000. **79**: p. 144-152.

76. Wenger, M.P., et al., *Mechanical properties of collagen fibrils.* Biophys J, 2007. **93**(4): p. 1255-63.

77. Mukherjee, A., et al., *Design of Fiber Networks for Studying Metastatic Invasion*, in *Biomechanics in Oncology*, C. Dong, N. Zahir, and K. Konstantopoulos, Editors. 2018, Springer International Publishing: Cham. p. 289-318.

78. Borghi, N., et al., *Regulation of cell motile behavior by crosstalk between cadherin-and integrin-mediated adhesions.* Proceedings of the National Academy of Sciences, 2010. **107**(30): p. 13324-13329.

79. Gottardi, C.J., E. Wong, and B.M. Gumbiner, *E-cadherin suppresses cellular transformation by inhibiting β-catenin signaling in an adhesion-independent manner.* The Journal of cell biology, 2001. **153**(5): p. 1049-1060.

80. Kovacs, E.M., R.G. Ali, and A.J. McCormack, *E-cadherin homophilic ligation directly signals through Rac and phosphatidylinositol 3-kinase to regulate adhesive contacts.* Journal of Biological Chemistry, 2002. **277**(8): p. 6708-6718.

81. Kovacs, E.M., et al., *Cadherin-Directed Actin Assembly: E-Cadherin Physically Associates with the Arp2/3 Complex to Direct Actin Assembly in Nascent Adhesive Contacts.* Current Biology, 2002. **12**(5): p. 379-382.

82. Biswas, K.H., et al., *E-cadherin junction formation involves an active kinetic nucleation process.* Proceedings of the National Academy of Sciences, 2015. **112**(35): p. 10932-10937.

83. Gavard, J., et al., *Lamellipodium extension and cadherin adhesion: two cell responses to cadherin activation relying on distinct signalling pathways.* Journal of Cell Science, 2004. **117**(2): p. 257-270.

84. Xu, W., et al., *Cell Stiffness Is a Biomarker of the Metastatic Potential of Ovarian Cancer Cells.* PLOS ONE, 2012. **7**(10): p. e46609.

85. Li, Q.S., et al., *AFM indentation study of breast cancer cells.* Biochem Biophys Res Commun, 2008. **374**(4): p. 609-13.

86. Lekka, M., et al., *Elasticity of normal and cancerous human bladder cells studied by scanning force microscopy.* European Biophysics Journal, 1999. **28**(4): p. 312-316.

87. Lekka, M., et al., *Cancer cell recognition – Mechanical phenotype.* Micron, 2012. **43**(12): p. 1259-1266.

88. Guo, X., et al., *The effect of neighboring cells on the stiffness of cancerous and non-cancerous human mammary epithelial cells.* New Journal of Physics, 2014. **16**(10).

89. Omidvar, R., et al., *Atomic force microscope-based single cell force spectroscopy of breast cancer cell lines: An approach for evaluating cellular invasion.* Journal of Biomechanics, 2014. **47**(13): p. 3373-3379.

90. Cross, S.E., et al., *AFM-based analysis of human metastatic cancer cells.* Nanotechnology, 2008. **19**(38): p. 384003.

91. Hjelm, H., K. Hjelm, and J. Sjöquist, *Protein A from Staphylococcus aureus. Its isolation by affinity chromatography and its use as an immunosorbent for isolation of immunoglobulins.* FEBS letters, 1972. **28**(1): p. 73-76.

92. Drees, F., A. Reilein, and W.J. Nelson, *Cell-adhesion assays: fabrication of an E-cadherin substratum and isolation of lateral and Basal membrane patches.* Methods Mol Biol, 2005. **294**: p. 303-20.

93. Kim, N.G., et al., *E-cadherin mediates contact inhibition of proliferation through Hippo signaling-pathway components.* Proc Natl Acad Sci U S A, 2011. **108**(29): p. 11930-5.

94. Dupont, S., et al., *Role of YAP/TAZ in mechanotransduction.* Nature, 2011. **474**(7350): p. 179.

95. Wada, K., et al., *Hippo pathway regulation by cell morphology and stress fibers.* Development, 2011. **138**(18): p. 3907-14.

96. De La Cruz, E.M. and E.M. Ostap, *Relating biochemistry and function in the myosin superfamily.* Current Opinion in Cell Biology, 2004. **16**(1): p. 61-67.

97. Nolen, B.J., et al., *Characterization of two classes of small molecule inhibitors of Arp2/3 complex.* Nature, 2009. **460**(7258): p. 1031-1034.

98. Holzinger, A., *Jasplakinolide: an actin-specific reagent that promotes actin polymerization.* Methods Mol Biol, 2009. **586**: p. 71-87.

99. Bubb, M.R., et al., *Jasplakinolide, a cytotoxic natural product, induces actin polymerization and competitively inhibits the binding of phalloidin to F-actin.* J Biol Chem, 1994. **269**(21): p. 14869-71.

# VITA

Mohamad Eftekharjoo

**Email:** mefte001@odu.edu **Cell:** 757-389-3413

## EDUCATION

- Ph.D. candidate in Mechanical Engineering (Spring 2016-Fall 2019)
  Old Dominion University, Norfolk, VA.
  Dissertation: The Effect of the Physical Micro-environment on Cell Adhesion and Force Exertion
- M.Sc. in Mechanical Engineering (Fall 2013-Fall 2015)
  Old Dominion University, Norfolk, VA.
  Thesis title: Multiple Point Constraint (MPC) - based Variable Node Super-element,
- B.Sc. in Industrial Engineering (2007-2011)
  Azad University south Tehran Branch, Tehran, Iran

## ADVANCED LABORATORY QUALIFICATIONS

- Proficient in growing different immortalized cell types (Endothelial, Epithelial, Fibroblasts, Cancerous) in variant *in vitro* cell culture mediums and systems using hydrogels, silicones and hard PDMS.
- Professional in characterizing mammalian tissue, and cancer cells (morphology, viability Cell-Cell and Cell-ECM communications) on how they respond to and mimic mechanical factors spatiotemporally through Cell Adhesions Molecules (CAMs) to their microenvironment.
- Expertise in coupling recombinant proteins onto substrates as well as implementing micropatterning techniques (using Quartz photomask or stainless steel sheet) for cells to adopt certain morphology at single or multicellular extent.
- Advanced knowledge of quantifying cellular force generation (single/island cells), implementing techniques such as Traction Force Microscopy (TFM), molecular DNA Tension Sensors, and actin retrograde flow.
- Expertise in cellular immunofluorescence staining at molecular level (Rhodamine, CY5, Phalloidin, DAPI).
- Solid knowledge of transient transfection techniques (Electroporation and reagent based) using constitutively active DNA and siRNA molecules to augment or attenuate the expression level of cellular molecules.
- Practical experienced in rheology of elastic substrates as well as implementing imaging techniques in order to characterize the substrate properties using spherical indentors.
- Advanced knowledge of Computational Finite Element Method (FEM) in solid structures.

## COMPUTER/LANGUAGE SKILLS

- Programing and Simulations: MATLAB, Mathematica, COMSOL (heat transfer models), NASTRAN (Basic), Design Expert (DX) (basic) and draftsight (basic)
- Data Analysis Software: ImageJ, Cell Profiler and Rheology (TA instrument TRIOS)
- Persian and English

## RESEARCH EXPERIENCE

- Cellular Mechanobiology laboratory (Spring 2016-Fall 2019)
- Thermo/Fluild laboratory (2014-2019): Conducting laboratory tests and operations.

- Wind tunnel laboratory (Summer 2014): Conducting aerodynamic tests.
- Iran- Khodro Diesel Factory as an intern (Summer 2010): Designing mechanical parts.

## PUBLICATIONS

- February 2019: Mohamad Eftekharjoo, Dakota Palmer, Breanna McCoy, Venkat Maruthamuthu: "*Fibrillar force generation by fibroblasts depends on formin*", Biochemical and Biophysical Research Communications 510 (2019) 72-77.
- (In progress- Will be submitted to PNAS) Mohamad Eftekharjoo, Siddharth chatterji and Venkat Maruthamuthu: *"E-cadherin biomimetic substrate for identifying E-Cadherin mechanosensitivity"*

## PRESENTATIONS

- Biomedical Engineering Society (BMES) October 2018, Mohamad Eftekharjoo and Venkat Maruthamuthu: "*The effect of substrate stiffness and formin on fibrillar force generation by fibroblasts*".
- Graduate Research Achievement Day (GRAD) spring 2019, Mohamad Eftekharjoo and Venkat Maruthamuthu: "*The effect of substrate stiffness and formin on fibrillar force generation by fibroblasts*".

## HONORS AND AWARDS

- Certified Graduate Teaching Assistant Instructor (GTAI) instructor (Spring 2017)
- An active member of Society of Manufacturing Engineering (SME) at ODU chapter-S113 (2015)

## MEMBERSHIPS

- Biomedical Engineering Society (BMES)
- Society of Manufacturing and Engineering (SME)